Published for SISSA by Springer

Received: May 13, 2022
Accepted: June 29, 2022
Published: August 2, 2022

A first glance to the kinematic moments of $B \to X_c \ell \nu$ at third order

Matteo Fael, Kay Schönwald and Matthias Steinhauser

Institut für Theoretische Teilchenphysik, Karlsruhe Institute of Technology (KIT), Wolfgang-Gaede Strasse 1, Karlsruhe 76128, Germany

E-mail: matteo.fael@kit.edu, kay.schoenwald@kit.edu, matthias.steinhauser@kit.edu

Abstract: We study the impact of third-order QCD corrections for several kinematic moments of the inclusive semileptonic B decays, to first order in the $1/m_b$ expansion. We consider the first four moments of the charged-lepton energy E_ℓ spectrum, the total leptonic invariant mass q^2 and the hadronic invariant mass M_X^2. No experimental cuts are applied. Our analytic results are obtained via an asymptotic expansion around the limit $m_b \simeq m_c$. After converting the scheme for the bottom mass to the kinetic scheme we compare the size of higher QCD corrections to the contributions from $1/m_b^2$ and $1/m_b^3$ power corrections and to the relative uncertainties.

Keywords: Higher-Order Perturbative Calculations, Semi-Leptonic Decays, Bottom Quarks

ArXiv ePrint: 2205.03410

https://doi.org/10.1007/JHEP08(2022)039

JHEP08(2022)039

Contents

JHEP08(2022)039

1 Introduction

Semileptonic B-meson decays mediated by the $b \to c\ell\bar{\nu}_\ell$ transition are sensitive to the absolute value of the Cabibbo-Kobayashi-Maskawa (CKM) matrix element V_{cb}. In the last years, measurements from BABAR, Belle and LHCb showed a puzzling discrepancy of about 3 standard deviations between the determinations of $|V_{cb}|$ from exclusive and inclusive decays [1]. A simultaneous resolution of the $|V_{cb}|$ (and $|V_{ub}|$) discrepancy is hardly possible in term of new physics [2]. Thus, further scrutiny of theoretical and experimental analyses are needed in order to shed light on the puzzle.

In this paper we focus on higher order QCD corrections to the kinematic moments of inclusive semileptonic $B \to X_c\ell\bar{\nu}_\ell$ decays. The theory underlying inclusive decays is based on a local operator product expansion, the Heavy Quark Expansion (HQE) [3–6], which allows to predict sufficiently inclusive decay observables, as the total semileptonic rate or moments of kinematic spectra, as an expansion in inverse powers of the bottom quark mass. In a first approximation, the process can be described as free quark decay. Bound-state effects are incorporated in a set of physical HQE parameters which appear starting at order $1/m_b^2$.

Inclusive kinematic distributions represent a portal to a precise determination of the HQE parameters and $|V_{cb}|$. Lepton energy moments and moments of hadronic invariant mass have been extensively measured at B factories and their prediction is know up to next-to-next-to leading order (NNLO) for free quarks [7–10], and next-to-leading order (NLO) at order $1/m_b^2$ [11–13]. Moments of the leptonic invariant mass have also received attention in the recent years due to their dependence on a smaller set of HQE parameters [14]. Results for the NLO corrections up to $1/m_b^3$ have been presented in [15].

It is the aim of this paper to compute the next-to-next-to-next-to-leading order ($\mathrm{N^3LO}$) corrections of kinematic moments and assess their relevance for the global fits of $|V_{cb}|$. Recently, we presented the $\mathrm{N^3LO}$ corrections to the semileptonic width [16] and the relation between the on-shell and kinetic mass of the bottom quark [17, 18]. In these works we took advantage of the heavy daughter expansion [19] to determine finite charm mass effects via an asymptotic expansion in the parameter $\delta = 1 - m_c/m_b$, where m_c and m_b are the charm and bottom masses, respectively. A similar strategy can be applied to compute moments in case no experimental cuts are applied, i.e. moments of kinematic distributions integrated over the whole phase space. We present in this work the first four moments of the charged-lepton energy E_ℓ, the total leptonic invariant mass q^2 and the hadronic invariant mass M_X^2. We study the behaviour of the perturbative series in the so-called kinetic scheme, in which the moments are expressed in terms of the kinetic mass of the bottom quark mass [17, 18, 20, 21]. Furthermore we estimate the theory uncertainty due to the finite expansion depth in δ.

We aim at validating the theoretical uncertainty estimates entering the $|V_{cb}|$ extraction and at identifying the precision level below which $\mathrm{N^3LO}$ corrections need to be taken into account. Usually, kinematic moments are measured with various kind of lower cuts on E_ℓ or q^2. On the one hand these cuts suppress background from low-energy electrons. On the other hand measurements with different cut values provide extra information on the HQE parameters. For a prediction of such kind of observables it is necessary to compute the differential rate to third order.

The paper is organized as follows. In section 2 we introduce the notation and present technical details of the calculation of the moments and also of the total rate presented in ref. [16]. We discuss in section 3 the numerical results in the on-shell scheme and discuss the theoretical uncertainties due to the finite expansion in the parameter δ. Numerical results in the kinetic scheme are given in section 4. NLO corrections to the power-suppressed terms of the q^2 moments are considered in section 5 and in section 6 we draw our conclusions. In the appendix we collect convenient formulae for one-loop integrals with arbitrary tensor rank and analytic expressions for the power-suppressed q^2 moments including perturbative one-loop corrections.

2 Details of the calculation

2.1 Moment definitions

We consider in perturbative QCD the inclusive decay of a bottom quark

$$b(p) \to X_c(p_x)\ell(p_\ell)\bar{\nu}_\ell(p_\nu), \tag{2.1}$$

JHEP08(2022)039

where X_c generically denotes a state containing a charm quark, plus additional gluons and/or quarks. In the rest frame of the bottom quark we have $p = (m_b, \vec{0})$. Leptons are considered to be massless. We denote the momentum of the lepton pair by $q = p_\ell + p_\nu$ and the total momentum of the hadronic system by $p_x = p - q$. In the following we study moments of the invariant mass q^2, the hadronic invariant mass M_X^2 and the charged-lepton energy E_ℓ. Moreover, quantities denoted by "$\hat{}$" refer to dimensionless quantities, normalized to the b quark mass, e.g. $\hat{q}^2 = q^2/m_b^2, \hat{E}_\ell = E_\ell/m_b$.

We compute moments of the differential rate where no restriction is applied on the final state particles. For their calculation we use the optical theorem in analogy to ref. [16] where the semileptonic width was presented. As building blocks it is convenient to introduce in the bottom quark rest frame the moments of the leptonic energy $q_0 = p \cdot q/m_b$ and the leptonic invariant mass q^2,

$$Q_{i,j} = \frac{1}{\Gamma_0} \int dE_\ell \, dq_0 \, dq^2 \, (q^2)^i (q_0)^j \frac{d^3\Gamma}{dE_\ell \, dq_0 \, dq^2}, \tag{2.2}$$

and moments of the charged-lepton energy $E_\ell = p_\ell \cdot p/m_b$

$$L_i = \frac{1}{\Gamma_0} \int dE_\ell \, dq_0 \, dq^2 \, (E_\ell)^i \frac{d^3\Gamma}{dE_\ell \, dq_0 \, dq^2} \tag{2.3}$$

with the normalization factor

$$\Gamma_0 = \frac{m_b^5 G_F^2 |V_{cb}|^2}{192\pi^3}. \tag{2.4}$$

Note that $Q_{0,0} = L_0$ corresponds to the total semileptonic rate computed in [16] (divided by Γ_0). Moments are written as a series expansion in the strong coupling constant $\alpha_s(\mu_s)$,

$$Q_{i,j} = \sum_{n\geq 0} Q_{i,j}^{(n)} \left(\frac{\alpha_s(\mu_s)}{\pi}\right)^n, \qquad L_i = \sum_{n\geq 0} L_i^{(n)} \left(\frac{\alpha_s(\mu_s)}{\pi}\right)^n. \tag{2.5}$$

Normalized moments are defined by

$$\langle (q^2)^n \rangle \equiv \frac{Q_{n,0}}{Q_{0,0}}, \qquad \langle E_\ell^n \rangle \equiv \frac{L_n}{L_0}, \tag{2.6}$$

with $n \geq 1$ and central moments are given by

$$\begin{aligned} q_1 &\equiv \langle q^2 \rangle, & q_n &\equiv \left\langle \left(q^2 - \langle q^2 \rangle\right)^n \right\rangle, \\ \ell_1 &\equiv \langle E_\ell \rangle, & \ell_n &\equiv \langle (E_\ell - \langle E_\ell \rangle)^n \rangle \, , \end{aligned} \tag{2.7}$$

where $n \geq 2$. Predictions for the central moments can be obtained by inserting the perturbative expansions (2.5) into (2.6) or (2.7) and re-expanding in α_s.

The hadronic invariant mass is related to parton level quantities by

$$M_X^2 \equiv (p_B - q)^2 = M_B^2 - 2M_B q_0 + q^2, \tag{2.8}$$

where p_B and M_B are the momentum and the mass of the B meson, respectively. We assume that the bottom quark and the B meson have the same velocity, i.e. $p_B^\mu = M_B v^\mu$

JHEP08(2022)039

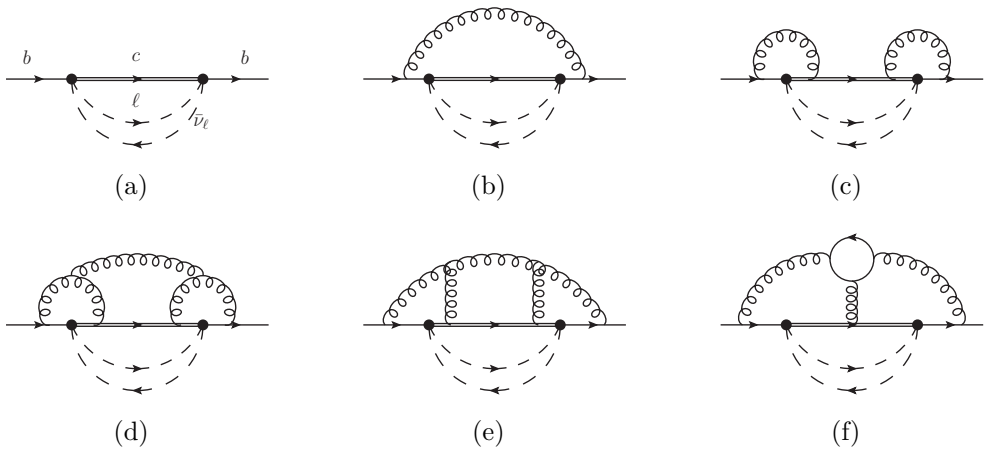

Figure 1. Sample Feynman diagrams which contribute to the forward scattering amplitude of a bottom quark at LO (a), NLO (b), NNLO (c) and $\mathrm{N^3LO}$ (d)–(f). Straight, curly and dashed lines represent quarks, gluons and leptons, respectively. The weak interaction mediated by the W boson is shown as a black dot.

and $p = m_b v^\mu$. The moments of M_X are given by linear combinations of the $Q_{i,j}$ moments:

$$\begin{aligned} M_n &= \frac{1}{\Gamma_0} \int dE_\ell \, dq_0 \, dq^2 \, (M_B^2 - 2M_B q_0 + q^2)^n \frac{d^3\Gamma}{dE_\ell \, dq_0 \, dq^2} \\ &= \sum_{i=0}^{n} \sum_{j=0}^{i} \binom{n}{i} \binom{i}{j} (M_B^2)^{n-i} (-2M_B)^{i-j} Q_{j,i-j} \,. \end{aligned} \tag{2.9}$$

Central moments are defined as

$$\langle (M_X^2)^n \rangle \equiv \frac{M_n}{M_0}, \qquad h_1 \equiv \langle M_X^2 \rangle, \qquad h_n \equiv \left\langle \left(M_X^2 - \langle M_X^2 \rangle \right)^n \right\rangle . \tag{2.10}$$

2.2 Asymptotic expansion

Let us now describe the calculation of $Q_{i,j}$ and L_i. With the help of the optical theorem we can express the $b \to X_c \ell \bar{\nu}_\ell$ matrix element integrated over the whole phase space in eqs. (2.2) and (2.3) in terms of the discontinuity of the $b \to b$ forward scattering amplitude (for sample Feynman diagrams see figure 1). Moments without cuts are simply obtained by multiplying the integrand of the forward scattering amplitude by the weight function $(q^2)^i (q \cdot v)^j$ or $(p_\ell \cdot v)^i$ for the $Q_{i,j}$ and L_i, respectively. The leading order prediction is obtained from the two-loop diagram in figure 1(a) where the internal lines correspond to the neutrino, the charged lepton and the charm quark. The weak interaction is shown as an effective vertex. To compute QCD corrections up to $O(\alpha_s^3)$ we have to add up to three more loops (see figure 1(b) to 1(f)).

An exact computation of five-loop diagrams with two mass scales (m_b and m_c) is out of range using current methods. We obtain finite charm mass effects by performing an asymptotic expansion in the parameter $\delta = 1 - m_c/m_b \ll 1$, i.e. we expand the Feynman diagrams around the equal mass limit $m_c \simeq m_b$, which we realize with the method of

JHEP08(2022)039

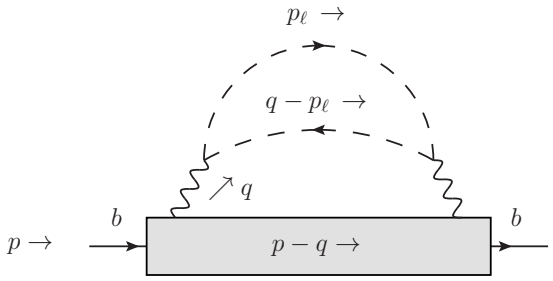

Figure 2. Our convention for the loop momentum routing. Charged lepton and neutrino momenta are p_ℓ and $q - p_\ell$, respectively. The external bottom quark momentum is p. Additional loops of gluons and quarks are denoted generically with the gray blob. The arrows on the fermion lines indicate the fermion direction whereas the arrows next to the lines denote the momentum flow.

regions [22, 23]. We call this approach the δ-*expansion*. The opposite limit $\rho = m_c/m_b \ll 1$ (the ρ-*expansion*) was adopted in [7] for the evaluation of the width to $O(\alpha_s^2)$.

It has been shown that the δ-expansion converges quite fast for the physical values of quark masses $\delta \simeq 0.7$ [16, 19, 24]. Moreover compared to an expansion around the opposite limit ($\rho \simeq 0.3$), the δ-expansion offers two crucial advantages:

1. The number of regions to be calculated is considerably smaller.

2. The δ-expansion yields a factorization of the multi-loop integrals which allows us to integrate at least two loop momenta without applying integration-by-part (IBP) relations. A computation up to $O(\alpha_s^n)$ becomes a n-loop problem, even if we start with $(n+2)$-loop Feynman diagrams.

In the following we elaborate on these two points. It is convenient to route the bottom quark momentum p along the external fermion line and we chose the momentum routing in the lepton-neutrino loop as shown in figure 2. Then the loop integrals w.r.t. p_ℓ take the form

$$I_1^{\mu_1\cdots\mu_N}(d, q^2; n_1, n_2) = \int \frac{d^d p_\ell}{(2\pi)^d} \frac{p_\ell^{\mu_1} \ldots p_\ell^{\mu_N}}{(-p_\ell^2)^{n_1}(-(p_\ell - q)^2)^{n_2}}, \tag{2.11}$$

where n_1 and n_2 are integers and $d = 4 - 2\epsilon$ is the space-time dimension. For such integrals one can derive a closed formula for arbitrary tensor rank N (see e.g. [23] and eq. (A.1) in appendix A). After performing the p_ℓ integration, we obtain integrals with an effective propagator $1/q^2$ raised to an ϵ-dependent power.

Next we apply the method of regions to construct the δ-expansion. There are only two possible scalings for each loop momentum k [23]:

- *hard* (h): $|k^\mu| \sim m_b$,
- *ultra-soft* (u): $|k^\mu| \sim \delta \cdot m_b = m_b - m_c$.

We choose the notion "ultra-soft" for the second scaling in analogy to the calculation of the relation between the pole and the kinetic mass of a heavy quark, see [17, 18]. For all

JHEP08(2022)039

diagrams, we checked with the program `asy.m` [25] that a naive scaling assignment to the individual loop momenta correctly identifies all relevant regions.

Since there is only one scale in the problem, the parameter δ (we set $m_b = 1$), an imaginary part arises only through the appearance of $\log(-\delta)$, i.e. only if δ appears in the denominator of one of the charm propagators. This implies that the combination $k - q$, where k is a loop momentum running through a charm quark line and $q = p_\ell + p_\nu$, must be ultra-soft for at least one of the charm propagators. Otherwise no imaginary part arises. Furthermore, the momentum q of the lepton pair always has to scale ultra-soft which means that all regions where q scales hard are discarded. To clarify this point, let us consider for instance the following propagator:

$$\frac{1}{(p-q+k)^2 - m_c^2} = \frac{1}{2p\cdot(k-q) + (k-q)^2 + 2\delta - \delta^2}, \tag{2.12}$$

where k denotes some generic linear combination of loop momenta other than q. If $k - q$ scales hard (p is considered always hard), we expand the charm propagators as follows

$$\frac{1}{(p-q+k)^2 - m_c^2} \overset{\text{h}}{=} \frac{1}{2p\cdot(k-q) + (k-q)^2} + O(\delta)\,. \tag{2.13}$$

Thus, no δ is left in the denominator and no imaginary part appears. If $k - q$ is ultra-soft we have

$$\frac{1}{(p-q+k)^2 - m_c^2} \overset{\text{u}}{=} \frac{1}{2p\cdot(k-q) + 2\delta} + O(\delta^0). \tag{2.14}$$

After integration the δ in the denominator yields a $\log(-\delta)$ term and thus an imaginary part.

At this point we exploit the fact that q is always ultra-soft which allows us to perform a further integration. Integrals where the loop momenta are hard factorize from the integration w.r.t. q. The crucial observation is that also in case q and k are both ultra-soft the integrations factorize. In fact, having chosen the momentum routing as in figure 2, the dependence in the charm propagators on q and δ is always of the form $(-2p\cdot q + 2\delta)$ as can be seen from eq. (2.14). Taking advantage of the linearity of the charm propagators in the ultra-soft region, we can pull out the global factor $(-2p\cdot q + 2\delta)$ from each propagator by rescaling the loop momenta. For instance, for the following two-loop integral we have[1]

$$\begin{aligned}\int \frac{d^dq\, d^dk}{(q^2)^{n_1}(k^2)^{n_2}(2p\cdot k - 2p\cdot q + 2\delta)^{n_3}} &\overset{k\to k(-2p\cdot q+2\delta)}{=} \\ &\int \frac{d^dq}{(q^2)^{n_1}(-2p\cdot q + 2\delta)^{-d+2n_2+n_3}} \times \int \frac{d^dk}{(k^2)^{n_2}(2p\cdot k + 1)^{n_3}}.\end{aligned} \tag{2.15}$$

Thus the q integration also factorizes for ultra-soft loop momentum k and therefore we can always evaluate the q-integration independently on the other loop momenta. The tensor integrals

$$I_2^{\mu_1\cdots\mu_N}(d,\delta,p^2;n_1,n_2) = \int \frac{d^dq}{(2\pi)^d} \frac{q^{\mu_1}\ldots q^{\mu_N}}{(-q^2)^{n_1}(-2p\cdot q + 2\delta)^{n_2}}, \tag{2.16}$$

[1] Note that we set $m_b = 1$.

JHEP08(2022)039

order	regions
α_s	u, h
α_s^2	**uu**, **hh**, hu
α_s^3	**uuu**, **hhh**, h**uu**, u**hh**

Table 1. Relevant regions for the loop momenta k_1, k_2, k_3 up to $O(\alpha_s^3)$: hard (h) and ultra-soft (u). Regions written in black factorize, leaving at most two- or three-loop integrals (in red) to be reduce by means of IBP relations.

can be directly evaluated using eq. (A.3) in appendix A. In conclusion, we are able to analytically carry out the integration w.r.t. p_ℓ and q without the need of an IBP reduction and we remain with n momentum integrations at order α_s^n. Each of these momenta can either be hard or ultra-soft.

With the same approach, it is possible to integrate all one-loop hard or ultra-soft contributions which leaves purely hard or ultra-soft integrals at two and three loops. We reduce them to master integrals via standard IBP reduction. We summarize all regions at order α_s, α_s^2 and α_s^3 in table 1. Those labeled in red required an IBP reduction, while the other regions factorize and are computed with the help of eqs. (A.1) to (A.3).

After asymptotic expansion of the Feynman integrals one gets linearly dependent propagators. It is thus necessary to perform a partial fraction decomposition in order to arrive at proper input expressions for the IBP reduction. The methods employed for the partial fraction decomposition and the mappings among different integral families closely follow those described in ref. [18], in particular we used the program `LIMIT` [26] to automate the partial fraction decomposition in case of linearly dependent denominators. For all cases where at least one of the regions is ultra-soft we can take over the master integrals from [17, 18]. For some of the (complicated) three-loop triple-ultra-soft master integrals, higher order ϵ terms are needed. The method used for their calculation and the results are given ref. [18]. All triple-hard master integrals can be found in ref. [27].

For all moments we have computed the first 16, 11 and 8 terms in the δ-expansion at order α_s, α_s^2 and α_s^3, respectively. Note that the leading power of δ is different for each moment:

$$\begin{aligned} \text{leading power of } \delta \text{ for } Q_{i,j}: &\quad \delta^{5+2i+j}, \\ \text{leading power of } \delta \text{ for } L_i: &\quad \delta^{5+i}. \end{aligned} \tag{2.17}$$

This means for example that the α_s^3 correction to the width is computed up to order δ^{12}, while for the third lepton energy moment L_3 the expansion extends to δ^{15}. Note that the leading term for the latter is δ^8.

The chosen expansion depths are a compromise between precision of our prediction and computational resources. To achieve sufficient precision, especially for the central moments (see next section), we had to perform a deep expansion in δ of the Feynman propagators, up to 8th or 10th order which has led to intermediate expressions of the order of 100 GB for each diagram. They must be handled carefully by `FORM` [28] in order to avoid an explosion of the number of terms.

JHEP08(2022)039

Furthermore for some of the integral families, individual propagators are raised to positive and negative powers up to 12, which constitute a non-trivial task for the IBP reduction programs. The latter could be handled thanks to a private version of `FIRE` [29] combined with `LiteRed` [30]. For the subset of integrals which are needed for the expansion up to δ^{10} we also use the stand-alone version of `LiteRed` as a cross-check.

There is an additional complication in the computation of the charged-lepton energy moments. They are computed by introducing the factor $(p_\ell \cdot v)^i$ in the integrand of the electron-neutrino loop, which make them dependent on the parity-odd part of the amplitude. As a consequence the traces which contain an odd number of γ_5 matrices does not cancel anymore and we have to deal with traces involving γ_5 in d dimension. We adopt the so-called Larin prescription [31] and substitute

$$\gamma^\mu\gamma^5 \to \frac{i}{3!}\,\varepsilon^{\mu\nu\rho\sigma}\,\frac{(\gamma_\nu\gamma_\rho\gamma_\sigma - \gamma_\sigma\gamma_\rho\gamma_\nu)}{2}\,, \tag{2.18}$$

in those cases where one instance of axial-vector current is present in a leptonic trace and one in the bottom-charm fermion line. After evaluating the traces of γ matrices, we contract the two Levi-Civita tensors and interpret the result in d dimensions. In case two γ_5 matrices are present in a trace, we simply anti-commute γ^5.

For the contributions where the Larin prescription have been used, an additional $\overline{\text{MS}}$ renormalization constant has to be taken into account. An axial-vector current treated with the Larin prescription must be renormalized with the factor [31, 32]

$$\begin{aligned} Z_A = 1 &+ \left(\frac{\alpha_s}{\pi}\right)^2 \frac{1}{\epsilon}\left(\frac{11}{24}C_A C_F - \frac{1}{6}C_F T_F n_f\right) + \left(\frac{\alpha_s}{\pi}\right)^3 \left[\frac{1}{\epsilon^2}\left(-\frac{121}{432}C_A^2 C_F + \frac{11}{54}C_A C_F T_F n_f + \right.\right. \\ &\left. - \frac{1}{27}C_F T_F^2 n_f^2\right) + \frac{1}{\epsilon}\left(\frac{1789}{2592}C_A^2 C_F - \frac{77}{144}C_A C_F^2 - \frac{26}{81}C_A C_F n_f T_F + \frac{1}{9}C_F^2 T_F n_f \right. \\ &\left.\left. + \frac{1}{162}C_F T_F^2 n_f^2\right)\right], \end{aligned} \tag{2.19}$$

where $T_F = 1/2$ is the trace normalization and $C_F = 4/3$ and $C_A = 3$ are the Casimir operators of the fundamental and the adjoint representation of SU(3), respectively, $\alpha_s \equiv \alpha_s^{(n_f)}(\mu_s)$, n_f is the number of active flavours and μ_s is the renormalization scale of the coupling constant. Furthermore one has to introduce a finite renormalization constant in order to restore the correct Ward identity:

$$\begin{aligned} Z_5 = 1 &- \frac{\alpha_s}{\pi}C_F + \left(\frac{\alpha_s}{\pi}\right)^2\left(-\frac{107}{144}C_A C_F + \frac{11}{8}C_F^2 + \frac{1}{36}C_F T_F n_f\right) \\ &+ \left(\frac{\alpha_s}{\pi}\right)^3\left[C_A^2 C_F\left(-\frac{2147}{1728} + \frac{7\zeta_3}{8}\right) + C_A C_F^2\left(\frac{2917}{864} - \frac{5\zeta_3}{2}\right) + C_F^3\left(-\frac{185}{96} + \frac{3\zeta_3}{2}\right)\right. \\ &\left. + C_A C_F T_F n_f\left(\frac{89}{648} + \frac{\zeta_3}{3}\right) + C_F^2 T_F n_f\left(-\frac{31}{432} - \frac{\zeta_3}{3}\right) + \frac{13}{324}C_F T_F^2 n_f^2\right]. \end{aligned} \tag{2.20}$$

Finally, it is interesting to note that the natural expansion parameter arising from the Feynman diagrams is actually $\delta' = 1 - m_c^2/m_b^2$ as odd powers of m_c do not appear in the differential rate because of the V–A weak interaction [33, 34]. Odd powers of m_c can

JHEP08(2022)039

appear in the lepton energy moments at intermediate steps when using the Larin scheme. In particular, they are present in the higher ϵ terms of the lower-order corrections. In this case we rewrite $m_c^{2n+1} = m_c(1-\delta')^n m_b^{2n}$ and treat m_c as additional parameter. However, after renormalization, we verify that all odd powers of m_c vanish.

The use of δ' further reduces the size of intermediate expressions. Only at the very end, after renormalization, we re-express our results in term of $\delta = 1-m_c/m_b = 1-\sqrt{1-\delta'}$ since the series in δ converges faster. This fact can be understood by comparing, for instance, the behaviour of the tree level decay rate which is proportional to the function

$$f(\rho) = 1 - 8\rho^2 + 8\rho^6 - \rho^8 - 12\rho^4 \log(\rho^2), \tag{2.21}$$

with $\rho = m_c/m_b$. If we substitute $\rho = 1-\delta$, at higher orders in δ the series is governed by the expansion of $\rho^4 \log(\rho^2)$ which is given by

$$\begin{aligned}\rho^4 \log(\rho^2) &= -2(1-\delta)^4 \log(1-\delta) = -2(1-\delta)^4 \sum_{m=1}^{\infty} \frac{\delta^m}{m} \\ &= -2\delta + 7\delta^2 - \frac{26}{3}\delta^3 + \frac{25}{6}\delta^4 - \sum_{n=5}^{\infty} \frac{48}{n(n-1)(n-2)(n-3)(n-4)}\delta^n. \end{aligned} \tag{2.22}$$

Instead, if we substitute $\rho^2 = 1-\delta'$ we obtain

$$\begin{aligned}\rho^4 \log(\rho^2) &= (1-\delta')^2 \log(1-\delta') = -(1-\delta')^2 \sum_{m=1}^{\infty} \frac{(\delta')^m}{m} \\ &= -\delta' + \frac{3}{2}(\delta')^2 - \sum_{n=3}^{\infty} \frac{2}{n(n-1)(n-2)}(\delta')^n \,. \end{aligned} \tag{2.23}$$

If we adopt δ as expansion parameter, the coefficients in the series are suppressed by $1/n^5$ for large n, while for δ' the coefficients are suppressed only by $1/n^3$. This fact suggest to use δ as expansion parameter also in the prediction at higher orders in α_s.

3 Results in the on-shell scheme

Our main results are analytic expressions for the moments $Q_{i,j}$ and L_i, with $i+j \leq 4$, which can be downloaded from [35]. In this section we first assess the uncertainty of the central moments related to the δ-expansion. In the next section we convert our results to the kinetic scheme and compare the size of the $O(\alpha_s^3)$ terms to experimental results and to the size of higher power corrections.

Let us fix for the numerical evaluation $m_b^{\rm OS} = 4.6\,\text{GeV}$ and $m_c^{\rm OS} = 1.15\,\text{GeV}$ which leads to $\delta = 0.75$. We use $M_B = 5.279\,\text{GeV}$ for the M_X^2 moments and set the renormalization scale $\mu_s = m_b^{\rm OS}$. The δ-expansion provides precise approximations for $Q_{i,j}$ and L_i. To give an idea of the convergence, we show the size of the different terms in the series at order α_s^3

JHEP08(2022)039

for three selected moments:

$$\begin{aligned}
\hat{Q}_{0,0}^{(3)} &= -44.9615(1_{\delta^5} - 0.527532_{\delta^6} + 4.38372_{\delta^7} - 2.54593_{\delta^8} + 0.102771_{\delta^9} \\
&\quad + 0.0168158_{\delta^{10}} + 0.00263043_{\delta^{11}} + 0.00216016_{\delta^{12}}), \\
\hat{Q}_{4,0}^{(3)} &= -0.703488(1_{\delta^{13}} - 0.527532_{\delta^{14}} + 2.79417_{\delta^{15}} - 1.488_{\delta^{16}} - 0.077824_{\delta^{17}} + \\
&\quad - 0.0329351_{\delta^{18}} - 0.0139737_{\delta^{19}} - 0.0058596_{\delta^{20}}), \\
\hat{L}_{1}^{(3)} &= -16.8605(1_{\delta^6} - 0.992521_{\delta^7} + 5.56695_{\delta^8} - 4.14032_{\delta^9} + 0.754176_{\delta^{10}} + \\
&\quad - 0.0251885_{\delta^{11}} - 0.0103673_{\delta^{12}} - 0.00171797_{\delta^{13}}),
\end{aligned} \tag{3.1}$$

where the subscripts are introduced to flag the different terms in the δ-expansion. The first equation corresponds to the expansion of the rate in [16]. We observe that at $O(\alpha_s^3)$ the precision reached with eight terms is well below the relative 1% level.

However, the accuracy on the central moments reduces. To compute central moments, we insert the analytic results of $L_i^{(n)}$ or $Q_{i,j}^{(n)}$ in eqs. (2.7) and (2.10) and re-expand in α_s to third order. The re-expansion in α_s of numerator and denominator is subject to strong cancellations. We do not re-expand in δ. The correction to central moments at order α_s^n involves non-trivial combinations of the moments $L_i^{(m)}$ or $Q_{i,j}^{(m)}$, where m ranges from 0 to n. A simple re-expansion in δ, let us say up to the eighth term at order α_s^3, spoils the delicate cancellations happening among different moments with $m < n$, which are actually computed to higher precision in δ. Therefore we suggest not to re-expand in δ quantities derived from $L_i^{(m)}$ or $Q_{i,j}^{(m)}$ since they represent the best possible approximation.

We estimate the final accuracy in the following way. We consider the moments with the highest computed term in δ and insert numerical values for the masses. Then we re-evaluate each moment removing the last term in the δ-expansion at each order in α_s. The difference between these two numerical predictions is quoted as uncertainty.

For the central q^2 moments normalized to m_b and expressed in the on-shell scheme we obtain

$$\begin{aligned}
\hat{q}_1 &= 0.218482 \left[1 + 0.127423\frac{\alpha_s}{\pi} + 0.4369(30)\left(\frac{\alpha_s}{\pi}\right)^2 - 5.34(30)\left(\frac{\alpha_s}{\pi}\right)^3\right], \\
\hat{q}_2 &= 0.0203994 \left[1 + 0.138093\frac{\alpha_s}{\pi} + 0.91584(89)\left(\frac{\alpha_s}{\pi}\right)^2 + 3.52(33)\left(\frac{\alpha_s}{\pi}\right)^3\right], \\
\hat{q}_3 &= 0.00110423 \left[1 - 0.226532\frac{\alpha_s}{\pi} + 1.137(14)\left(\frac{\alpha_s}{\pi}\right)^2 + 53.37(59)\left(\frac{\alpha_s}{\pi}\right)^3\right], \\
\hat{q}_4 &= 0.000889517 \left[1 + 0.167677\frac{\alpha_s}{\pi} + 1.5921(11)\left(\frac{\alpha_s}{\pi}\right)^2 + 15.24(35)\left(\frac{\alpha_s}{\pi}\right)^3\right].
\end{aligned} \tag{3.2}$$

For the E_ℓ moments we find

$$\begin{aligned}
\hat{\ell}_1 &= 0.307202 \left[1 - 0.0169117\frac{\alpha_s}{\pi} - 0.6637(30)\left(\frac{\alpha_s}{\pi}\right)^2 - 15.01(15)\left(\frac{\alpha_s}{\pi}\right)^3\right], \\
\hat{\ell}_2 &= 0.00862693 \left[1 - 0.164901\frac{\alpha_s}{\pi} - 2.0568(59)\left(\frac{\alpha_s}{\pi}\right)^2 - 35.4(2.9)\left(\frac{\alpha_s}{\pi}\right)^3\right],
\end{aligned}$$

JHEP08(2022)039

$$\hat{\ell}_3 = -0.00041875\left[1 - 0.00580025\frac{\alpha_s}{\pi} - 1.4848(68)\left(\frac{\alpha_s}{\pi}\right)^2 - 25(17)\left(\frac{\alpha_s}{\pi}\right)^3\right],$$
$$\hat{\ell}_4 = 0.000189369\left[1 - 0.245899\frac{\alpha_s}{\pi} - 3.534(28)\left(\frac{\alpha_s}{\pi}\right)^2 - 76(481)\left(\frac{\alpha_s}{\pi}\right)^3\right]. \quad (3.3)$$

For M_X^2 moments it is more convenient to normalize the results w.r.t. the first order in α_s since the partonic X_c invariant mass differs from m_c only starting at $O(\alpha_s)$ due to real radiation. Our results read

$$\hat{h}_1 = 0.0993848\left[2.10166 + 1\frac{\alpha_s}{\pi} + 14.567(25)\left(\frac{\alpha_s}{\pi}\right)^2 + 249.0(2.4)\left(\frac{\alpha_s}{\pi}\right)^3\right],$$
$$\hat{h}_2 = 0.0150817\left[0.029471 + 1\frac{\alpha_s}{\pi} + 11.098(59)\left(\frac{\alpha_s}{\pi}\right)^2 + 152(40)\left(\frac{\alpha_s}{\pi}\right)^3\right],$$
$$\hat{h}_3 = 0.00342142\left[-0.00103783 + 1\frac{\alpha_s}{\pi} + 9.27(21)\left(\frac{\alpha_s}{\pi}\right)^2 + 201(24)\left(\frac{\alpha_s}{\pi}\right)^3\right],$$
$$\hat{h}_4 = 0.001168\left[0.000361694 + 1\frac{\alpha_s}{\pi} + 9.1(1.4)\left(\frac{\alpha_s}{\pi}\right)^2 + 0(19)\times 10^3\left(\frac{\alpha_s}{\pi}\right)^3\right]. \quad (3.4)$$

We notice that the central q_i moments are well approximated by the δ-expansion. The uncertainties of the α_s^3 coefficients are at most of about 10%. For the first three E_ℓ and M_X central moments, we find that our approximation is able to determine the size of the third order correction. However for the moments $\hat{\ell}_4$ and $\hat{h}_4$ we observe that our expansion depth is not deep enough and the large uncertainty is a consequence of severe numerical cancellations.

We noticed also that an uncertainty estimate based on standard error propagation in general overestimates the uncertainty. If we assigned to each moment $L_i^{(m)}$ and $Q_{i,j}^{(m)}$ an error equal to the last known term in δ and then combine the uncertainties in an uncorrelated way, we would find for $\hat{q}_i$ and $\hat{\ell}_i$ uncertainties much larger than those quoted above. For hadronic moments we would observe errors of similar size. This fact is likely connected to stronger correlations among the different expansion terms in δ for the q^2 and E_ℓ moments.

We compared our results at $\mathcal{O}(\alpha_s^2)$ with the values for the M_X and E_ℓ moments of refs. [9, 10] and find good agreement.

4 Transition to the kinetic scheme

In this section we discuss the impact of higher order QCD corrections once a short-distance mass scheme is adopted. Moreover we will compare them to the power corrections at order $1/m_b^2$ and $1/m_b^3$ to understand the importance of the α_s^3 corrections in the fits for $|V_{cb}|$.

In this work we concentrate on the so called *kinetic scheme* employed in the fits of refs. [6, 36, 37]. In this scheme we adopt the kinetic mass [17, 18, 20, 21] for the bottom

JHEP08(2022)039

quark using

$$m_b^{\rm kin}(\mu) = m_b^{\rm OS} - [\overline{\Lambda}(\mu)]_{\rm pert} - \frac{[\mu_\pi^2(\mu)]_{\rm pert}}{2m_b^{\rm kin}(\mu)} - O\left(\frac{1}{(m_b^{\rm kin})^2}\right), \tag{4.1}$$

while the charm quark mass is converted to the $\overline{\rm MS}$ scheme. At the same time, in the kinetic scheme one redefines the heavy-quark-expansion parameters μ_π^2 and ρ_D^3 in the following way:

$$\mu_\pi^2(0) = \mu_\pi^2(\mu) - [\mu_\pi^2(\mu)]_{\rm pert}, \qquad \rho_D^3(0) = \rho_D^3(\mu) - [\rho_D^3(\mu)]_{\rm pert}, \tag{4.2}$$

where the analytic expressions for $[\overline{\Lambda}(\mu)]_{\rm pert}$, $[\mu_\pi^2(\mu)]_{\rm pert}$ and $[\rho_D^3(\mu)]_{\rm pert}$ can be found in the appendix of ref. [18]. The Wilsonian cutoff μ plays the role of scale separation between the short- and long-distance regimes. We adopt the standard HQE parameter definitions employed in refs. [4, 36, 37]:

$$\begin{aligned}
\mu_\pi^2 &= -\frac{1}{2M_B}\langle B|\,\bar b_v (iD^\perp)^2 b_v\,|B\rangle\,,\\
\mu_G^2 &= \frac{1}{2M_B}\langle B|\,\bar b_v (iD_\mu^\perp)(iD_\nu^\perp)(-i\sigma^{\mu\nu}) b_v\,|B\rangle\,,\\
\rho_D^3 &= \frac{1}{2M_B}\langle B|\,\bar b_v (iD_\mu^\perp)(iv\cdot D)(iD^{\perp\nu}) b_v\,|B\rangle\,,\\
\rho_{LS}^3 &= \frac{1}{2M_B}\langle B|\,\bar b_v (iD_\mu^\perp)(iv\cdot D)(iD_\nu^\perp)(-i\sigma^{\mu\nu}) b_v\,|B\rangle\,,
\end{aligned} \tag{4.3}$$

where $D_\mu = \partial_\mu - ig_s A_\mu$, $D_\mu^\perp = (g_{\mu\nu} - v_\mu v_\nu)(iD^\nu)$, $b_v(x) = \exp(-im_b v\cdot x) b(x)$. The B meson velocity and mass are denoted by $v^\mu = p_B^\mu/m_B$ and m_B, respectively.

We consider two different approaches for the construction of the central moments:

(A) As a first step, expressions for central moments are obtained in the on-shell scheme. To this end, the ratios in eqs. (2.7) and (2.10) are expanded up to $O(\alpha_s^3)$ (to leading order in $1/m_b$) and up to $1/m_b^3$ for the power corrections. We discard higher α_s corrections in the sub-leading power in $1/m_b$. Afterwards one applies the transition to the kinetic scheme.

(B) We convert the expressions for $Q_{i,j}$ and L_i to the kinetic scheme. In a second step the ratios in eqs. (2.7) and (2.10) are expanded up to α_s^3 (to leading order in $1/m_b$) and up to $O(1/m_b^3)$ for the power corrections.

Note that the two approaches do not yield the same analytic expressions because of the redefinition of the HQE parameters, see eq. (4.2). In approach (A) the perturbative versions of μ_π and ρ_D appear after expanding the central moments in α_s and $1/m_b$. In case (B) they are introduced before expansion, and therefore treated as α_s corrections in the later re-expansion of the ratios. Approach (A) and (B) start to differ at order α_s^2 since the shift of the power-suppressed terms according to eq. (4.2) induces perturbative α_s corrections from $1/m_b$ terms. In both approaches, we retain all powers of the Wilsonian cutoff $\mu/m_b^{\rm kin}$.

JHEP08(2022)039

Only those terms involving one of the genuine non-perturbative parameters are expanded in $1/m_b$. For a further discussion of the differences between the two approaches and their interpretation we refer to section 5 where $\mathcal{O}(\alpha_s)$ corrections to power-suppressed terms are considered for the q^2 moments.

We set the renormalization scale of the strong coupling constant $\mu_s = m_b^{\rm kin}$ and use $\alpha_s^{(4)}(m_b^{\rm kin})$ as expansion parameter, i.e. we decouple the bottom quark from the running of α_s, and we re-expand in $\alpha_s^{(4)}$ up to third order. We use the input values

$$\begin{aligned} m_b^{\rm kin}(1\,{\rm GeV}) &= 4.526\,{\rm GeV}, & \overline{m}_c(3\,{\rm GeV}) &= 0.993\,{\rm GeV}, \\ \mu &= 1\,{\rm GeV}, & \alpha_s^{(4)}(m_b^{\rm kin}) &= 0.2186. \end{aligned} \tag{4.4}$$

For the HQE parameters, we use the most updated values and their correlations from [37]:

$$\begin{aligned} \mu_\pi^2 &= 0.477(56)\,{\rm GeV}^2, & \rho_D^3 &= 0.185(31)\,{\rm GeV}^3, \\ \mu_G^2 &= 0.306(50)\,{\rm GeV}^2, & \rho_{LS}^3 &= -0.130(92)\,{\rm GeV}^3, \end{aligned} \tag{4.5}$$

where all parameters are defined at $\mu = 1\,{\rm GeV}$.

In the following we report the numerical prediction for the various moments in the kinetic scheme, employing approaches (A) and (B). For each moment we factorize out the tree-level prediction, and show the size of the α_s, α_s^2 and α_s^3 corrections (denoted by $X_{\alpha_s^n}$). The quoted uncertainties come from the δ expansion as explained in the previous section. We denote the sum of all $1/m_b^2$ and $1/m_b^3$ corrections by the subscript "pw".

For comparison, we quote also an uncertainty for the contribution of higher $1/m_b$ corrections. It arises from the uncertainties in the HQE parameters given in eq. (4.5) with correlations taken into account. We will use this uncertainty as reference value to compare the relevance of the α_s^3 corrections in the fits for $|V_{cb}|$.

4.1 q^2 moments

We first show results for the q^2 moments with approach (A)

$$\begin{aligned} \hat{q}_1 &= 0.232947\left[1 - 0.0106345_{\alpha_s} - 0.008736(15)_{\alpha_s^2} - 0.00505(13)_{\alpha_s^3} - 0.0875(97)_{\rm pw}\right], \\ \hat{q}_2 &= 0.0235256\left[1 - 0.035937_{\alpha_s} - 0.0217035(20)_{\alpha_s^2} - 0.01118(17)_{\alpha_s^3} - 0.237(27)_{\rm pw}\right], \\ \hat{q}_3 &= 0.0014511\left[1 - 0.0700381_{\alpha_s} - 0.035693(73)_{\alpha_s^2} - 0.01909(12)_{\alpha_s^3} - 0.726(94)_{\rm pw}\right], \\ \hat{q}_4 &= 0.00120161\left[1 - 0.0585199_{\alpha_s} - 0.042276(11)_{\alpha_s^2} - 0.02411(20)_{\alpha_s^3} - 0.631(77)_{\rm pw}\right]. \end{aligned} \tag{4.6}$$

With approach (B) we obtain:

$$\begin{aligned} \hat{q}_1 &= 0.232947\left[1 - 0.0106332_{\alpha_s} - 0.007100(16)_{\alpha_s^2} - 0.00326(13)_{\alpha_s^3} - 0.0875(97)_{\rm pw}\right], \\ \hat{q}_2 &= 0.0235256\left[1 - 0.0359328_{\alpha_s} - 0.0175591(28)_{\alpha_s^2} - 0.00677(17)_{\alpha_s^3} - 0.237(27)_{\rm pw}\right], \\ \hat{q}_3 &= 0.00145109\left[1 - 0.0700256_{\alpha_s} - 0.030529(71)_{\alpha_s^2} - 0.01282(12)_{\alpha_s^3} - 0.726(94)_{\rm pw}\right], \\ \hat{q}_4 &= 0.0012016\left[1 - 0.0585099_{\alpha_s} - 0.0342994(88)_{\alpha_s^2} - 0.01597(20)_{\alpha_s^3} - 0.631(77)_{\rm pw}\right]. \end{aligned} \tag{4.7}$$

JHEP08(2022)039

For the q^2 moments we observe a good behaviour of the perturbative series, with coefficients precisely determined via the δ-expansion. Note that for the q^2 moments, even α_s^2 corrections are not yet available in the literature as the results presented in refs. [9, 10] are only for electron energy and hadronic invariant mass moments.

The size of the α_s^2 corrections are of few percent while third order corrections are about a factor of two smaller and in the range of 0.5–2%. We observe that higher power corrections are sizable and as large as 70% of the leading order contribution. The estimated uncertainty of the power corrections are a factor two to three larger compared to the α_s^3 term. At $O(\alpha_s^3)$ the difference between the two approaches yields a difference of $0.3\%, 0.9\%, 1.1\%$ and 1.6% for the four moments which is of the same order of magnitude as the α_s^3 terms.

Central moments of the q^2 spectrum have been measured recently by Belle [38] separately for electrons and muons in the final state. The quoted results for a cut on the leptonic invariant mass of $q^2 > 3\,\text{GeV}^2$, averaged between muon and electron, read[2]

$$\begin{aligned} q_1(q^2 > 3\,\text{GeV}^2) &= 6.23\,(8)\,\text{GeV}^2, \\ q_2(q^2 > 3\,\text{GeV}^2) &= 4.44\,(15)\,\text{GeV}^4, \\ q_3(q^2 > 3\,\text{GeV}^2) &= 4.13\,(68)\,\text{GeV}^6, \\ q_4(q^2 > 3\,\text{GeV}^2) &= 46.6\,(5.6)\,\text{GeV}^8\,. \end{aligned} \tag{4.8}$$

Due to the cut of q^2 we refrain from a direct comparison to our predictions. However, it is interesting to compare the uncertainties. The moments in eq. (4.8) have a relative uncertainty of $1.3\%, 3.1\%, 16\%$ and 12%. The experimental error of q_1 and q_2 is only about a factor two larger compared to the magnitude of the α_s^3 term. Furthermore, note that the measurements in [38] with a higher cut on q^2 have even smaller uncertainties reaching a precision of 0.5% which makes the α_s^3 corrections even more relevant.

4.2 Charged-lepton energy moments

For the electron energy moments our result in the approach (A) read

$$\begin{aligned} \hat{\ell}_1 &= 0.315615\left[1 - 0.0101064_{\alpha_s} - 0.005082(17)_{\alpha_s^2} - 0.00227(13)_{\alpha_s^3} - 0.0192(31)_{\text{pw}}\right], \\ \hat{\ell}_2 &= 0.00900585\left[1 - 0.01992_{\alpha_s} - 0.006152(41)_{\alpha_s^2} + 0.0002(21)_{\alpha_s^3} + 0.017(11)_{\text{pw}}\right], \\ \hat{\ell}_3 &= -0.000464269\left[1 - 0.0639319_{\alpha_s} - 0.035673(10)_{\alpha_s^2} - 0.0142(46)_{\alpha_s^3} - 0.175(22)_{\text{pw}}\right], \\ \hat{\ell}_4 &= 0.00020743\left[1 - 0.028854_{\alpha_s} - 0.00717(23)_{\alpha_s^2} - 0.00(25)_{\alpha_s^3} + 0.000(21)_{\text{pw}}\right], \end{aligned} \tag{4.9}$$

while for (B) we find

$$\begin{aligned} \hat{\ell}_1 &= 0.315615\left[1 - 0.010106_{\alpha_s} - 0.004838(17)_{\alpha_s^2} - 0.00200(13)_{\alpha_s^3} - 0.0192(31)_{\text{pw}}\right], \\ \hat{\ell}_2 &= 0.00900585\left[1 - 0.0199202_{\alpha_s} - 0.006303(42)_{\alpha_s^2} - 0.0001(21)_{\alpha_s^3} + 0.017(11)_{\text{pw}}\right], \\ \hat{\ell}_3 &= -0.000464268\left[1 - 0.0639261_{\alpha_s} - 0.0358480(91)_{\alpha_s^2} - 0.0142(46)_{\alpha_s^3} - 0.175(22)_{\text{pw}}\right], \\ \hat{\ell}_4 &= 0.00020743\left[1 - 0.0288534_{\alpha_s} - 0.00611(23)_{\alpha_s^2} + 0.00(25)_{\alpha_s^3} + 0.000(21)_{\text{pw}}\right]. \end{aligned} \tag{4.10}$$

[2]We thank F. Bernlochner and R. van Tonder for providing us with the values of the central moments constructed from the data of ref. [38].

JHEP08(2022)039

For these moments we observe in general a good convergence of the perturbative series in the kinetic scheme. It is interesting to note that the relative size of the α_s^3 corrections are smaller compared to those found for q^2 moments. For $\hat{\ell}_1$ and $\hat{\ell}_2$ we have 0.2% and 0.02% and for $\hat{\ell}_3$ about 1.4%. For $\hat{\ell}_4$, the α_s^3 correction is not determined in a reliable way due to the uncertainty of the finite expansion in δ. On the other hand, also the impact of the power corrections is much smaller compared to q^2 moments. For $\hat{\ell}_1$ and $\hat{\ell}_2$ the power correction uncertainty is of the order of 0.1–0.3% and comparable with the size of α_s^3 corrections. The α_s^3 coefficient of $\hat{\ell}_2$ is small which is likely due to numerical cancellation. In case of $\hat{\ell}_3$ the uncertainty coming from higher $1/m_b$ terms of about 2.2% is comparable with the α_s^3 correction.

The difference between our predictions obtained with the approaches (A) and (B) are small, and overall they never exceed the 0.1% of the leading order contribution.

We can examine the precision of experimental measurements for instance by quoting the values of the electron energy moments, with a cut $E_\ell > 0.4\,\text{GeV}$, as measure by Belle [39]

$$\begin{aligned}
\ell_1(E_\ell > 0.4\,\text{GeV}) &= 1393.92(6.73)(3.02)\,\text{MeV},\\
\ell_2(E_\ell > 0.4\,\text{GeV}) &= 168.77(3.68)(1.53)\times 10^{-3}\,\text{GeV}^2,\\
\ell_3(E_\ell > 0.4\,\text{GeV}) &= -21.04(1.93)(0.66)\times 10^{-3}\,\text{GeV}^3,\\
\ell_4(E_\ell > 0.4\,\text{GeV}) &= 64.153(1.813)(0.935)\times 10^{-3}\,\text{GeV}^4.
\end{aligned} \tag{4.11}$$

The relative accuracies of these measurements are 0.5%, 2.3%, 9.6% and 3.2%, respectively. Due to the applied cut, the central values cannot directly be compared to our prediction. However, we note that for $\hat{\ell}_1$ the α_s^3 corrections are only a factor of two smaller than the experimental error. Also for the moments of the charged lepton energy, the experimental measurements are in general more precise at higher values of the cut. Therefore for some of the moments, third order QCD corrections are already comparable to the experimental error and the uncertainties associated to power corrections.

4.3 Hadronic invariant mass moments

Finally let us analyze the predictions for the hadronic invariant mass moments. For approach (A) we have

$$\begin{aligned}
\hat{h}_1 &= 0.00899843\left[+23.4975 + 1 + 0.4223(15)_{\alpha_s^2} + 0.147(11)_{\alpha_s^3} + 0.04(20)_{\text{pw}}\right],\\
\hat{h}_2 &= 0.000745468\left[+0.87352 + 1 + 0.4505(74)_{\alpha_s^2} + 0.34(43)_{\alpha_s^3} + 3.33(59)_{\text{pw}}\right],\\
\hat{h}_3 &= 0.0000915954\left[-0.0729568 + 1 + 0.165(62)_{\alpha_s^2} + 2.29(55)_{\alpha_s^3} + 7.3(1.1)_{\text{pw}}\right],\\
\hat{h}_4 &= 0.000091207\left[+0.0100938 + 1 + 0.51(17)_{\alpha_s^2} + 1(145)_{\alpha_s^3} + 0.380(52)_{\text{pw}}\right],
\end{aligned} \tag{4.12}$$

while for (B) we find

$$\begin{aligned}
\hat{h}_1 &= 0.00899836\left[+23.4976 + 1 + 0.4114(15)_{\alpha_s^2} + 0.134(11)_{\alpha_s^3} + 0.04(20)_{\text{pw}}\right],\\
\hat{h}_2 &= 0.000745462\left[+0.873533 + 1 + 0.3971(73)_{\alpha_s^2} + 0.25(43)_{\alpha_s^3} + 3.33(59)_{\text{pw}}\right],
\end{aligned}$$

JHEP08(2022)039

$$\hat{h}_3 = 0.0000915935\left[-0.0729428 + 1 - 0.088(61)_{\alpha_s^2} + 2.00(55)_{\alpha_s^3} + 7.3(1.1)_{\rm pw}\right],$$
$$\hat{h}_4 = 0.0000912064\left[+0.0100992 + 1 + 0.56(16)_{\alpha_s^2} + 0(145)_{\alpha_s^3} + 0.380(52)_{\rm pw}\right]. \quad (4.13)$$

As before, we normalize the various higher order terms w.r.t. the $O(\alpha_s)$ corrections, since the partonic tree-level invariant mass vanishes.

Our approximation does not determine $\hat{h}_4$ at $O(\alpha_s^3)$ and also for $\hat{h}_2$ we can only provide the order of magnitude. While for $\hat{h}_1$ and $\hat{h}_2$ the perturbative series still displays a good convergence, the prediction for $\hat{h}_3$ shows an enhanced $O(\alpha_s^3)$ term which is more than a factor of two larger than the $O(\alpha_s)$ contribution. For $\hat{h}_3$ also the power-suppressed terms are quite large and the corresponding uncertainty is as large as the $O(\alpha_s)$ term. This calls for a careful assessment of the theoretical uncertainties for this specific moment, or as a conservative approach, for the elimination of $\hat{h}_3$ from the set of observables considered in the fits. For $\hat{h}_1$ the relative difference between approaches (A) and (B) is about 0.1% while for $\hat{h}_2$ and $\hat{h}_3$ it is of 2.3% and 5%, respectively.

From the expressions in eq. (4.13) we obtain after multiplication with the proper power of m_b the results

$$\begin{aligned} h_1 &= 4.628(36)(2)\,\text{GeV}^2 = 4.63(4)\,\text{GeV}^2, \\ h_2 &= 1.88(23)(31)\,\text{GeV}^4 = 1.88(40)\,\text{GeV}^4, \\ h_3 &= 8.41(0.97)(1.73)\,\text{GeV}^6 = 8.4(2.0)\,\text{GeV}^6. \end{aligned} \quad (4.14)$$

We observe from eq. (4.12) and (4.13) that the theory prediction is dominated by the power-suppressed terms for h_2 and h_3. The first kind of uncertainties quoted in (4.14) reflects only the parametric uncertainties on the values of the HQE parameters in eq. (4.5) and those from the truncation of the expansion in δ, which are added in quadrature. The second kind of uncertainty is an estimate of the missing higher-order terms in the $1/m_b$ expansion, i.e. $O(1/m_b^4)$ or higher, which are likely sizable for h_2 and h_3. We estimated this additional source of uncertainty as 30% of the power-suppressed contributions in eq. (4.12) and (4.13). We refrain from listing h_4 since there is a strong dependence on the higher order power-suppressed corrections [40].

The results in eq. (4.14) can be compared to the experimental measurements of the M_X moments performed by DELPHI [41]:[3]

$$\begin{aligned} h_1 &= 4.541\,(101)\,\text{GeV}^2, \\ h_2 &= 1.56\,(18)\,(16)\,\text{GeV}^4, \\ h_3 &= 4.05\,(74)\,(32)\,\text{GeV}^6. \end{aligned} \quad (4.15)$$

Note that no cuts have been applied. Their relative errors are 2%, 15% and 20%, respectively. For h_1 one observes agreement within the uncertainties. Note, however, that the experimental error is about a factor 2.5 larger than the one from the theory prediction. Furthermore, from eq. (4.13) one observes that the contribution from the α_s^3 term has

[3] We thank P. Gambino for clarification about the value of h_1.

JHEP08(2022)039

about the same order of magnitude as the theory uncertainty. Also for h_2 we find agreement between the theory prediction and the experimental result. For h_3 the agreement is at the 2σ level. In case we neglect the uncertainty from higher order $1/m_b^4$ terms in the theory prediction, we would observe a 3.5σ tension in h_3. In the case of h_3 it is worth to mention that the expansion in α_s does not converge and therefore it becomes questionable if the HQE is applicable at all in this case. Moreover, for h_2 and h_3 we observe that the α_s^3 terms are larger than the quoted error by DELPHI.

5 Including NLO perturbative corrections to the power suppressed terms

In this section we study the origin in the numerical differences between approach (A) and (B), and how it can be reduced by including NLO perturbative corrections to the power suppressed terms, i.e. by taking into account $O(\alpha_s)$ corrections in the Wilson coefficients of the HQE parameters $\mu_\pi^2, \mu_G^2, \rho_D^3$ and ρ_{LS}^3. We will refer to these correction as α_s/m_b^n corrections ($n = 2$ or 3 in our case).

We focus on the q^2 moments. Analytic results for the q^2 spectrum including α_s/m_b^n corrections were recently computed in [15]. By performing an analytic integration of the differential decay rate, we obtain expressions for the perturbative corrections to power suppressed terms of the q^2 moments. Schematically they have the form (compare also with eq. (2.5))

$$\begin{aligned} Q_{i,0} = &\left[Q_{i,0}^{(0)} + Q_{i,0}^{(1)}\frac{\alpha_s}{\pi} + Q_{i,0}^{(2)}\left(\frac{\alpha_s}{\pi}\right)^2 + Q_{i,0}^{(3)}\left(\frac{\alpha_s}{\pi}\right)^3\right]\left(1 - \frac{\mu_\pi^2}{2m_b^2}\right) + Q_{i,0,\mu_G}^{(0)}\left(\frac{\mu_G^2}{m_b^2} - \frac{\rho_{LS}^3}{m_b^3}\right) \\ &+ Q_{i,0,\mu_G}^{(1)}\frac{\alpha_s}{\pi}\frac{\mu_G^2}{m_b^2} + Q_{i,0,\rho_{LS}}^{(1)}\frac{\alpha_s}{\pi}\frac{\rho_{LS}^3}{m_b^3} + \left[Q_{i,0,\rho_D}^{(0)} + Q_{i,0,\rho_D}^{(1)}\frac{\alpha_s}{\pi}\right]\frac{\rho_D^3}{m_b^3}\,, \end{aligned} \tag{5.1}$$

where $\alpha_s \equiv \alpha_s(\mu_s)$. For convenience we provide analytic results for $Q_{i,0,\mu_G}^{(0)}$, $Q_{i,0,\mu_G}^{(1)}$ and $Q_{i,0,\rho_{LS}}^{(1)}$ in appendix B. The results for $Q_{i,0,\rho_D}^{(0)}$ and $Q_{i,0,\rho_D}^{(1)}$ can be found in ref. [15].

Let us compare the predictions for the central moments q_i obtained in eqs. (33) and (34) where no $O(\alpha_s/m_b^n)$ correction was taken into account. We obtain

$$\begin{aligned} \Delta q_1 &= 0.3\%, \\ \Delta q_2 &= 0.9\%, \\ \Delta q_3 &= 1.1\%, \\ \Delta q_4 &= 1.6\%, \end{aligned} \tag{5.2}$$

where we define the relative difference between scheme (A) and (B) by

$$\Delta q_i \equiv \frac{|\hat{q}_i^{(A)} - \hat{q}_i^{(B)}|}{\hat{q}_i^{\rm LO}}. \tag{5.3}$$

Let us explain the origin of such difference. It is related to terms of the form

$$\alpha_s \times \frac{\rho_D^3}{m_b^3}. \tag{5.4}$$

JHEP08(2022)039

In the kinetic scheme one has to redefine $\rho_D^3(0)$ according to eq. (4.2) where the perturbative expansion of $[\rho_D(\mu)]_{\rm pert}$ is given by

$$[\rho_D^3(\mu)]_{\rm pert} = \mu^3 \sum_{n\geq 1} r_{\rm pert}^{(n)} \left(\frac{\alpha_s}{\pi}\right)^n . \tag{5.5}$$

The coefficients $r_{\rm pert}^{(n)}$ are known up to $O(\alpha_s^3)$ from [18]. Their explicit expressions are not relevant for our discussion. For q^2 moments we can ignore the role of μ_π^2 since its dependence drops out due to reparametrization invariance [14].

In case we neglect terms of $O(\alpha_s/m_b^n)$, contributions scaling like $\alpha_s \times \rho_D^3/m_b^3$ are dropped in approach (A) after re-expansion of (2.7) in the on-shell scheme. In approach (B) we first transform the building blocks entering eq. (2.7) to the kinetic scheme. In particular, we redefine ρ_D^3 according to eq. (4.2). After inserting the expressions in eq. (2.7) and expanding in α_s new terms of order α_s^2 are generated since the ratio μ^3/m_b^3 is considered of order one and not $1/m_b^3$. Thus, we observe that the difference between (A) and (B) scales like $\alpha_s^2 r_{\rm pert}^{(1)} \mu^3/m_b^3$ if $O(\alpha_s/m_b^n)$ terms are neglected. In case α_s/m_b^n terms are included the difference is of order $\alpha_s^2 r_{\rm pert}^{(1)} \mu^6/m_b^6$.

We now compare the values of the q^2 moments obtained in approaches (A) and (B) after the inclusion of terms of $O(\alpha_s/m_b^n)$. We recompute the prediction for the central moments q_i by re-expanding the final result up to $O(\alpha_s^3)$ at the partonic level, while we keep corrections of $O(\alpha_s/m_b^n)$ in the power suppressed terms. With approach (A) we obtain

$$\begin{aligned}
\hat{q}_1 &= 0.232947 \left[1 - 0.0106137_{\alpha_s} - 0.00383463_{\alpha_s^2} - 0.00327(13)_{\alpha_s^3} - 0.097(11)_{\rm pw}\right], \\
\hat{q}_2 &= 0.0235256 \left[1 - 0.0359242_{\alpha_s} - 0.00697531_{\alpha_s^2} - 0.00683(17)_{\alpha_s^3} - 0.240(27)_{\rm pw}\right], \\
\hat{q}_3 &= 0.0014511 \left[1 - 0.0701143_{\alpha_s} + 0.0145548_{\alpha_s^2} - 0.00866(13)_{\alpha_s^3} - 0.624(80)_{\rm pw}\right], \\
\hat{q}_4 &= 0.00120161 \left[1 - 0.058515_{\alpha_s} - 0.000100666_{\alpha_s^2} - 0.01686(20)_{\alpha_s^3} - 0.545(65)_{\rm pw}\right],
\end{aligned} \tag{5.6}$$

and approach (B) leads to

$$\begin{aligned}
\hat{q}_1 &= 0.232947 \left[1 - 0.0106265_{\alpha_s} - 0.00402646_{\alpha_s^2} - 0.00190(13)_{\alpha_s^3} - 0.094(11)_{\rm pw}\right], \\
\hat{q}_2 &= 0.0235256 \left[1 - 0.0359104_{\alpha_s} - 0.00817945_{\alpha_s^2} - 0.00366(17)_{\alpha_s^3} - 0.227(26)_{\rm pw}\right], \\
\hat{q}_3 &= 0.00145109 \left[1 - 0.0699819_{\alpha_s} + 0.00342844_{\alpha_s^2} - 0.00822(12)_{\alpha_s^3} - 0.510(68)_{\rm pw}\right], \\
\hat{q}_4 &= 0.0012016 \left[1 - 0.0584734_{\alpha_s} - 0.00681918_{\alpha_s^2} - 0.01185(20)_{\alpha_s^3} - 0.477(58)_{\rm pw}\right].
\end{aligned} \tag{5.7}$$

Taking the difference from leading m_b contribution only, i.e., from the terms flagged by "α_s^i" we obtain

$$\begin{aligned}
\Delta q_1 &= 0.1\%, \\
\Delta q_2 &= 0.2\%, \\
\Delta q_3 &= 1.1\%, \\
\Delta q_4 &= 0.2\%.
\end{aligned} \tag{5.8}$$

JHEP08(2022)039

Comparing eqs. (5.8) and (5.2) we observe that the predictions using (A) and (B) get closer after the inclusion of the $O(\alpha_s/m_b^n)$ corrections. This happens because now both approach (A) and (B) take into account contributions scaling as $\alpha_s \times \rho_D^3/m_b^3$. After redefinition of ρ_D, both (A) and (B) generate the same corrections of the form $\alpha_s^2 r_{\rm pert}^{(1)} \mu^3/m_b^3$. Therefore Δq_i become smaller.

However if we take into account also the power-suppressed terms, i.e., the parts flagged by "pw", we obtain

$$\begin{aligned} \Delta q_1 &= 0.4\%, \\ \Delta q_2 &= 1.5\%, \\ \Delta q_3 &= 10.3\%, \\ \Delta q_4 &= 6.6\%, \end{aligned} \tag{5.9}$$

which are even larger than without including $O(\alpha_s/m_b^n)$ terms. Similarly to what we observed before, the difference starts now at order $1/m_b^2$ and $1/m_b^3$ because of contributions of the form

$$\alpha_s \times \frac{[\rho_D^3]_{\rm pert}}{m_b^3} \times \frac{\mu_G^2}{m_b^2} \quad \text{or} \quad \alpha_s \times \frac{[\rho_D^3]_{\rm pert}}{m_b^3} \times \frac{\rho_D^3(\mu)}{m_b^3} \tag{5.10}$$

which arise if one uses approach (B). However these terms are actually of $O(1/m_b^5)$ and $O(1/m_b^6)$ and therefore they would not appear if $[\rho_D]_{\rm pert}/m_b^3 \sim \mu^3/m_b^3$ is considered as a $1/m_b^3$ suppressed term and the expressions for the moments re-expanded up to $1/m_b^3$.

In the end, we conclude that the ambiguity between approaches (A) and (B) can be removed if the power corrections μ/m_b originating from the kinetic scheme are considered as $1/m_b$ suppressed term in the HQE. Note that for the charged-lepton energy moments the contribution from the power-suppressed terms are significantly smaller and thus the different treatment of the μ/m_b terms is numerically less important as can be seen from the comparison of eqs. (4.9) and (4.10).

6 Conclusions

In this work we compute several kinematic moments of inclusive $B \to X_c \ell \bar{\nu}_\ell$ decays up to $O(\alpha_s^3)$. In particular we consider for the first time higher order QCD corrections to q^2 moments. We use the optical theorem to obtain analytic expressions for the moments as an expansion in the parameter $\delta = 1 - m_c/m_b$. For most of the considered observables, the series expansion in δ is sufficient to obtain precise results for the coefficients of the perturbative expansion. However, for some of the central moments, there are significant cancellations and our finite expansion depth in δ does not allow for a determination of the α_s^3 corrections in a reliable way. Note that also a calculation based on numerical methods might have similar problems since also there in a first step the elementary moments are computed with a finite numerical accuracy [10].

We describe in detail our computational methods. The quark masses are renormalized in the on-shell scheme. Afterwards, we study the moments in the kinetic scheme and investigate the importance of the higher order QCD corrections for the determination of $|V_{cb}|$. To this end, we present numerical results in the kinetic scheme together with the contribution from higher $1/m_b$ power corrections and the related uncertainties.

JHEP08(2022)039

For the first two q^2 and electron energy moments, we find that the third order corrections are of the same order as the uncertainties associated to $1/m_b^2$ and $1/m_b^3$ corrections. Furthermore, they are comparable in size with experimental errors. Thus, the inclusion of α_s^3 corrections in future analyses might be important. For the hadronic invariant mass moments $\hat{h}_2$ and $\hat{h}_3$ we observe α_s^3 corrections which are of the same order of magnitude or even larger than experimental uncertainties and thus might influence the $|V_{cb}|$ fit. For these moments also the power-suppressed terms are sizeable.

We discuss two approaches for the construction of the central moments in the kinetic scheme. In approach (A) the scheme transformation rules are applied to the central moments in the on-shell scheme. On the other hand, in approach (B) the building blocks are transformed to the kinetic scheme and the central moments are constructed afterwards. The numerical results differ starting from order α_s^2 which is due to the fact that μ/m_b counts as order one, where μ is the Wilsonian cutoff of the kinetic scheme. For the q^2 we show that the difference reduces in case higher order QCD corrections to the power-suppressed terms are considered.

The analysis of the inclusive third order corrections of charged-lepton energy, leptonic invariant mass and hadronic invariant mass moments performed in this paper suggests that one should initiate a differential calculations at third order.

Acknowledgments

We kindly thank Alexander Smirnov for providing us with the development version of `FIRE`. We also thank Joshua Davies for many useful hints on the efficient treatment of large expressions with `FORM`. Furthermore, we are grateful to Paolo Gambino for useful comments to the manuscript. Feynman diagrams were drawn with the help of Axodraw [42] and JaxoDraw [43]. This research was supported by the Deutsche Forschungsgemeinschaft (DFG, German Research Foundation) under grant 396021762 — TRR 257 "Particle Physics Phenomenology after the Higgs Discovery".

A Tensor decomposition formulas

In this appendix we report the formulas employed to compute one-loop hard and ultra-soft tensor integrals. We denote by $\{[g]^r[p]^{N-2r}\}^{\mu_1\dots\mu_N}$ the product of r metric tensors and $N-2r$ vectors p, totally symmetric in its N Lorentz indices.

A.1 Massless two-point integral

The tensor integral of a massless one-loop two-point function is given by (see e.g. ref. [23])

$$\int \frac{d^dk}{(2\pi)^d} \frac{k^{\mu_1}\dots k^{\mu_N}}{(-k^2)^{n_1}(-(k-q))^{n_2}} = \frac{i}{(4\pi)^{d/2}}(-q^2)^{d/2-n_1-n_2}$$
$$\times \sum_{r=0}^{[N/2]} \frac{\Gamma(n_1+n_2-r-d/2)\Gamma(d/2+N-n_1-r)\Gamma(d/2-n_2+r)}{2^r\Gamma(n_1)\Gamma(n_2)\Gamma(d+N-n_1-n_2)}(q^2)^r\{[g]^r[q]^{N-2r}\}^{\mu_1\dots\mu_N}, \tag{A.1}$$

where $[N/2]$ is the greatest integer less than or equal to $N/2$.

JHEP08(2022)039

A.2 On-shell two-point integral with one mass

The tensor integral of a massive one-loop two-point function reads

$$\int \frac{d^dk}{(2\pi)^d}\frac{k^{\mu_1}\dots k^{\mu_N}}{(-k^2)^{n_1}(-k^2+2p\cdot k)^{n_2}} = \frac{i}{(4\pi)^{d/2}}(m^2)^{d/2-n_1-n_2} \times \sum_{r=0}^{[N/2]}\frac{\Gamma(n_1+n_2-r-d/2)\Gamma(d+N-2n_1-n_2)}{(-2)^r\Gamma(n_2)\Gamma(d+N-n_1-n_2)}(m^2)^r\{[g]^r[p]^{N-2r}\}^{\mu_1\dots\mu_N} \tag{A.2}$$

where $p^2=m^2$. Such integrals appear in case the loop momentum is hard.

A.3 Ultra-soft integral

The tensor integral of a one-loop ultra-soft two-point function is given by

$$\int \frac{d^dk}{(2\pi)^d}\frac{k^{\mu_1}\dots k^{\mu_N}}{(-k^2)^{n_1}(-2p\cdot k+y)^{n_2}} = \frac{i}{(4\pi)^{d/2}}y^{d-2n_1-n_2+N}(p^2)^{n_1-N-d/2} \times \sum_{r=0}^{[N/2]}\frac{(-1)^{N+r}\Gamma(d/2-n_1-r+N)\Gamma(2n_1+n_2-N-d)}{2^r\Gamma(n_1)\Gamma(n_2)}(p^2)^r\{[g]^r[p]^{N-2r}\}^{\mu_1\dots\mu_N}. \tag{A.3}$$

B Inclusive q^2 moments to order α_s

The analytic results for the leading m_b expansion terms read

$$\begin{aligned}Q_{0,0}^{(1)} = C_F\Bigg\{&\frac{25}{8}-\frac{239\tilde\rho}{6}+\frac{239\tilde\rho^3}{6}-\frac{25\tilde\rho^4}{8}+\ln(\tilde\rho)\Big(-10\tilde\rho-45\tilde\rho^2+\frac{2\tilde\rho^3}{3}-\frac{17\tilde\rho^4}{6}\\&+64\tilde\rho^{3/2}(1+\tilde\rho)\ln\left(1+\sqrt{\tilde\rho}\right)\Big)+\ln(1-\tilde\rho)\Big[-\frac{17}{6}+\frac{32\tilde\rho}{3}-\frac{32\tilde\rho^3}{3}+\frac{17\tilde\rho^4}{6}\\&+\Big(2+60\tilde\rho^2+2\tilde\rho^4-32\tilde\rho^{3/2}-32\tilde\rho^{5/2}\Big)\ln(\tilde\rho)\Big]+\pi^2\Big(-\frac{1}{2}-8\tilde\rho^2-\frac{\tilde\rho^4}{2}+16\tilde\rho^{3/2}\\&+16\tilde\rho^{5/2}\Big)-\frac{1}{2}\tilde\rho^2(36+\tilde\rho^2)\ln^2(\tilde\rho)-128\tilde\rho^{3/2}(1+\tilde\rho)\mathrm{Li}_2(\sqrt{\tilde\rho})+(3+48\tilde\rho^2+3\tilde\rho^4\\&+32\tilde\rho^{3/2}+32\tilde\rho^{5/2})\mathrm{Li}_2(\tilde\rho)\Bigg\},\end{aligned} \tag{B.1}$$

$$\begin{aligned}Q_{1,0}^{(1)} = C_F\Bigg\{&\frac{39}{40}-\frac{17117\tilde\rho}{600}-\frac{139129\tilde\rho^2}{900}+\frac{139129\tilde\rho^3}{900}+\frac{17117\tilde\rho^4}{600}-\frac{39\tilde\rho^5}{40}\\&+\ln(1-\tilde\rho)\Big[-\frac{301}{300}+\frac{185\tilde\rho}{36}+\frac{50\tilde\rho^2}{3}-\frac{50\tilde\rho^3}{3}-\frac{185\tilde\rho^4}{36}+\frac{301\tilde\rho^5}{300}+\ln(\tilde\rho)\Big(\frac{3}{5}+\frac{\tilde\rho}{3}\\&+110\tilde\rho^2+110\tilde\rho^3+\frac{\tilde\rho^4}{3}+\frac{3\tilde\rho^5}{5}-32\tilde\rho^{3/2}-\frac{2368}{15}\tilde\rho^{5/2}-32\tilde\rho^{7/2}\Big)\Big]+\ln(\tilde\rho)\Big[-\frac{123\tilde\rho}{20}+\end{aligned}$$

JHEP08(2022)039

$$
\begin{aligned}
&-\frac{3251\tilde{\rho}^2}{30}-\frac{917\tilde{\rho}^3}{10}-\frac{91\tilde{\rho}^4}{90}-\frac{301\tilde{\rho}^5}{300}+\left(64\tilde{\rho}^{3/2}+\frac{4736}{15}\tilde{\rho}^{5/2}+64\tilde{\rho}^{7/2}\right)\ln\left(1+\sqrt{\tilde{\rho}}\right)\Big]\\
&+\pi^2\Big(-\frac{3}{20}-\frac{\tilde{\rho}}{12}-16\tilde{\rho}^2-16\tilde{\rho}^3-\frac{\tilde{\rho}^4}{12}-\frac{3\tilde{\rho}^5}{20}+16\tilde{\rho}^{3/2}+\frac{1184}{15}\tilde{\rho}^{5/2}+16\tilde{\rho}^{7/2}\Big)\\
&+\mathrm{Li}_2(\tilde{\rho})\Big(\frac{9}{10}+\frac{\tilde{\rho}}{2}+96\tilde{\rho}^2+96\tilde{\rho}^3+\frac{\tilde{\rho}^4}{2}+\frac{9\tilde{\rho}^5}{10}+32\tilde{\rho}^{3/2}+\frac{2368}{15}\tilde{\rho}^{5/2}+32\tilde{\rho}^{7/2}\Big)+\\
&-\left(27\tilde{\rho}^2+35\tilde{\rho}^3+\frac{\tilde{\rho}^4}{12}+\frac{3\tilde{\rho}^5}{20}\right)\ln^2(\tilde{\rho})-\left(128\tilde{\rho}^{3/2}+\frac{9472}{15}\tilde{\rho}^{5/2}+128\tilde{\rho}^{7/2}\right)\mathrm{Li}_2\left(\sqrt{\tilde{\rho}}\right)\Big\},
\end{aligned}
\tag{B.2}
$$

$$
\begin{aligned}
Q^{(1)}_{2,0}=C_F\Big\{&\frac{302}{675}-\frac{21247\tilde{\rho}}{900}-\frac{85018\tilde{\rho}^2}{225}+\frac{85018\tilde{\rho}^4}{225}+\frac{21247\tilde{\rho}^5}{900}-\frac{302\tilde{\rho}^6}{675}\\
&+\ln(1-\tilde{\rho})\Big[-\frac{112}{225}+\frac{763\tilde{\rho}}{225}+\frac{280\tilde{\rho}^2}{9}-\frac{280\tilde{\rho}^4}{9}-\frac{763\tilde{\rho}^5}{225}+\frac{112\tilde{\rho}^6}{225}+\ln(\tilde{\rho})\Big(\frac{4}{15}\\
&+\frac{4\tilde{\rho}}{15}+\frac{476\tilde{\rho}^2}{3}+\frac{1400\tilde{\rho}^3}{3}+\frac{476\tilde{\rho}^4}{3}+\frac{4\tilde{\rho}^5}{15}+\frac{4\tilde{\rho}^6}{15}-32\tilde{\rho}^{3/2}-\frac{5408}{15}\tilde{\rho}^{5/2}-\frac{5408}{15}\tilde{\rho}^{7/2}+\\
&-32\tilde{\rho}^{9/2}\Big)\Big]+\ln(\tilde{\rho})\Big[-\frac{68\tilde{\rho}}{15}-\frac{933\tilde{\rho}^2}{5}-\frac{2132\tilde{\rho}^3}{5}-\frac{6997\tilde{\rho}^4}{45}-\frac{257\tilde{\rho}^5}{225}-\frac{112\tilde{\rho}^6}{225}\\
&+\ln\left(1+\sqrt{\tilde{\rho}}\right)\left(64\tilde{\rho}^{3/2}+\frac{10816}{15}\tilde{\rho}^{5/2}+\frac{10816}{15}\tilde{\rho}^{7/2}+64\tilde{\rho}^{9/2}\right)\Big]+\mathrm{Li}_2\left(\sqrt{\tilde{\rho}}\right)\Big(-128\tilde{\rho}^{3/2}+\\
&-\frac{21632}{15}\tilde{\rho}^{5/2}-\frac{21632}{15}\tilde{\rho}^{7/2}-128\tilde{\rho}^{9/2}\Big)+\pi^2\Big(-\frac{1}{15}-\frac{\tilde{\rho}}{15}-\frac{71\tilde{\rho}^2}{3}-\frac{640\tilde{\rho}^3}{9}-\frac{71\tilde{\rho}^4}{3}+\\
&-\frac{\tilde{\rho}^5}{15}-\frac{\tilde{\rho}^6}{15}+16\tilde{\rho}^{3/2}+\frac{2704}{15}\tilde{\rho}^{5/2}+\frac{2704}{15}\tilde{\rho}^{7/2}+16\tilde{\rho}^{9/2}\Big)+\mathrm{Li}_2(\tilde{\rho})\Big(\frac{2}{5}+\frac{2\tilde{\rho}}{5}+142\tilde{\rho}^2\\
&+\frac{1280\tilde{\rho}^3}{3}+142\tilde{\rho}^4+\frac{2\tilde{\rho}^5}{5}+\frac{2\tilde{\rho}^6}{5}+32\tilde{\rho}^{3/2}+\frac{5408}{15}\tilde{\rho}^{5/2}+\frac{5408}{15}\tilde{\rho}^{7/2}+32\tilde{\rho}^{9/2}\Big)\\
&+\left(-36\tilde{\rho}^2-\frac{380\tilde{\rho}^3}{3}-\frac{155\tilde{\rho}^4}{3}-\frac{\tilde{\rho}^5}{15}-\frac{\tilde{\rho}^6}{15}\right)\ln^2(\tilde{\rho})\Big\},
\end{aligned}
\tag{B.3}
$$

$$
\begin{aligned}
Q^{(1)}_{3,0}=C_F\Big\{&\frac{1243}{5040}-\frac{724597\tilde{\rho}}{35280}-\frac{38846267\tilde{\rho}^2}{58800}-\frac{174182263\tilde{\rho}^3}{176400}+\frac{174182263\tilde{\rho}^4}{176400}\\
&+\frac{38846267\tilde{\rho}^5}{58800}+\frac{724597\tilde{\rho}^6}{35280}-\frac{1243\tilde{\rho}^7}{5040}+\ln^2(\tilde{\rho})\Big(-45\tilde{\rho}^2-300\tilde{\rho}^3-\frac{1359\tilde{\rho}^4}{4}-\frac{273\tilde{\rho}^5}{4}+\\
&-\frac{\tilde{\rho}^6}{20}-\frac{\tilde{\rho}^7}{28}\Big)+\ln(1-\tilde{\rho})\Big[-\frac{851}{2940}+\frac{763\tilde{\rho}}{300}+\frac{917\tilde{\rho}^2}{20}+\frac{665\tilde{\rho}^3}{12}-\frac{665\tilde{\rho}^4}{12}-\frac{917\tilde{\rho}^5}{20}+\\
&-\frac{763\tilde{\rho}^6}{300}+\frac{851\tilde{\rho}^7}{2940}+\ln(\tilde{\rho})\Big(\frac{1}{7}+\frac{\tilde{\rho}}{5}+207\tilde{\rho}^2+1197\tilde{\rho}^3+1197\tilde{\rho}^4+207\tilde{\rho}^5+\frac{\tilde{\rho}^6}{5}+\frac{\tilde{\rho}^7}{7}+
\end{aligned}
$$

JHEP08(2022)039

$$
\begin{aligned}
&- 32\tilde{\rho}^{3/2} - 640\tilde{\rho}^{5/2} - \frac{51264}{35}\tilde{\rho}^{7/2} - 640\tilde{\rho}^{9/2} - 32\tilde{\rho}^{11/2}\Big)\Big] + \ln(\tilde{\rho})\Big[-\frac{101\tilde{\rho}}{28} - \frac{38707\tilde{\rho}^2}{140} + \\
&- \frac{126527\tilde{\rho}^3}{105} - \frac{482833\tilde{\rho}^4}{420} - \frac{8072\tilde{\rho}^5}{35} - \frac{1117\tilde{\rho}^6}{1050} - \frac{851\tilde{\rho}^7}{2940} + \ln\left(1+\sqrt{\tilde{\rho}}\right)\Big(64\tilde{\rho}^{3/2} \\
&+ 1280\tilde{\rho}^{5/2} + \frac{102528}{35}\tilde{\rho}^{7/2} + 1280\tilde{\rho}^{9/2} + 64\tilde{\rho}^{11/2}\Big)\Big] + \mathrm{Li}_2\big(\sqrt{\tilde{\rho}}\big)\Big(-128\tilde{\rho}^{3/2} - 2560\tilde{\rho}^{5/2} + \\
&- \frac{205056}{35}\tilde{\rho}^{7/2} - 2560\tilde{\rho}^{9/2} - 128\tilde{\rho}^{11/2}\Big) + \pi^2\Big(-\frac{1}{28} - \frac{\tilde{\rho}}{20} - \frac{125\tilde{\rho}^2}{4} - \frac{743\tilde{\rho}^3}{4} + \\
&- \frac{743\tilde{\rho}^4}{4} - \frac{125\tilde{\rho}^5}{4} - \frac{\tilde{\rho}^6}{20} - \frac{\tilde{\rho}^7}{28} + 16\tilde{\rho}^{3/2} + 320\tilde{\rho}^{5/2} + \frac{25632}{35}\tilde{\rho}^{7/2} + 320\tilde{\rho}^{9/2} + 16\tilde{\rho}^{11/2}\Big) \\
&+ \mathrm{Li}_2(\tilde{\rho})\Big(\frac{3}{14} + \frac{3\tilde{\rho}}{10} + \frac{375\tilde{\rho}^2}{2} + \frac{2229\tilde{\rho}^3}{2} + \frac{2229\tilde{\rho}^4}{2} + \frac{375\tilde{\rho}^5}{2} + \frac{3\tilde{\rho}^6}{10} + \frac{3\tilde{\rho}^7}{14} + 32\tilde{\rho}^{3/2} \\
&+ 640\tilde{\rho}^{5/2} + \frac{51264}{35}\tilde{\rho}^{7/2} + 640\tilde{\rho}^{9/2} + 32\tilde{\rho}^{11/2}\Big)\Big\}, \qquad \text{(B.4)}
\end{aligned}
$$

$$
\begin{aligned}
Q^{(1)}_{4,0} = C_F\Big\{&\frac{1429}{9408} - \frac{970901\tilde{\rho}}{52920} - \frac{175592549\tilde{\rho}^2}{176400} - \frac{313385041\tilde{\rho}^3}{88200} + \frac{313385041\tilde{\rho}^5}{88200} \\
&+ \frac{175592549\tilde{\rho}^6}{176400} + \frac{970901\tilde{\rho}^7}{52920} - \frac{1429\tilde{\rho}^8}{9408} + \ln^2(\tilde{\rho})\Big(-54\tilde{\rho}^2 - 580\tilde{\rho}^3 - \frac{3773\tilde{\rho}^4}{3} + \\
&- \frac{3536\tilde{\rho}^5}{5} - \frac{424\tilde{\rho}^6}{5} - \frac{4\tilde{\rho}^7}{105} - \frac{3\tilde{\rho}^8}{140}\Big) + \ln(1-\tilde{\rho})\Big[-\frac{5449}{29400} + \frac{7508\tilde{\rho}}{3675} + \frac{4592\tilde{\rho}^2}{75} \\
&+ \frac{12628\tilde{\rho}^3}{75} - \frac{12628\tilde{\rho}^5}{75} - \frac{4592\tilde{\rho}^6}{75} - \frac{7508\tilde{\rho}^7}{3675} + \frac{5449\tilde{\rho}^8}{29400} + \ln(\tilde{\rho})\Big(\frac{3}{35} + \frac{16\tilde{\rho}}{105} + \frac{1276\tilde{\rho}^2}{5} \\
&+ \frac{12144\tilde{\rho}^3}{5} + 4774\tilde{\rho}^4 + \frac{12144\tilde{\rho}^5}{5} + \frac{1276\tilde{\rho}^6}{5} + \frac{16\tilde{\rho}^7}{105} + \frac{3\tilde{\rho}^8}{35} - 32\tilde{\rho}^{3/2} - \frac{14944}{15}\tilde{\rho}^{5/2} + \\
&- \frac{141504}{35}\tilde{\rho}^{7/2} - \frac{141504}{35}\tilde{\rho}^{9/2} - \frac{14944}{15}\tilde{\rho}^{11/2} - 32\tilde{\rho}^{13/2}\Big)\Big] + \ln(\tilde{\rho})\Big[-3\tilde{\rho} - \frac{39449\tilde{\rho}^2}{105} + \\
&- \frac{280199\tilde{\rho}^3}{105} - \frac{2987011\tilde{\rho}^4}{630} - \frac{437533\tilde{\rho}^5}{175} - \frac{165101\tilde{\rho}^6}{525} - \frac{3517\tilde{\rho}^7}{3675} - \frac{5449\tilde{\rho}^8}{29400} \\
&+ \ln\left(1+\sqrt{\tilde{\rho}}\right)\Big(64\tilde{\rho}^{3/2} + \frac{29888}{15}\tilde{\rho}^{5/2} + \frac{283008}{35}\tilde{\rho}^{7/2} + \frac{283008}{35}\tilde{\rho}^{9/2} + \frac{29888}{15}\tilde{\rho}^{11/2} \\
&+ 64\tilde{\rho}^{13/2}\Big)\Big] + \mathrm{Li}_2\big(\sqrt{\tilde{\rho}}\big)\Big(-128\tilde{\rho}^{3/2} - \frac{59776}{15}\tilde{\rho}^{5/2} - \frac{566016}{35}\tilde{\rho}^{7/2} - \frac{566016}{35}\tilde{\rho}^{9/2} + \\
&- \frac{59776}{15}\tilde{\rho}^{11/2} - 128\tilde{\rho}^{13/2}\Big) + \pi^2\Big(-\frac{3}{140} - \frac{4\tilde{\rho}}{105} - \frac{194\tilde{\rho}^2}{5} - \frac{5708\tilde{\rho}^3}{15} - \frac{6776\tilde{\rho}^4}{9} + \\
&- \frac{5708\tilde{\rho}^5}{15} - \frac{194\tilde{\rho}^6}{5} - \frac{4\tilde{\rho}^7}{105} - \frac{3\tilde{\rho}^8}{140} + 16\tilde{\rho}^{3/2} + \frac{7472}{15}\tilde{\rho}^{5/2} + \frac{70752}{35}\tilde{\rho}^{7/2} + \frac{70752}{35}\tilde{\rho}^{9/2}
\end{aligned}
$$

JHEP08(2022)039

$$+\frac{7472}{15}\tilde{\rho}^{11/2}+16\tilde{\rho}^{13/2}\Big)+\mathrm{Li}_2(\tilde{\rho})\Big(\frac{9}{70}+\frac{8\tilde{\rho}}{35}+\frac{1164\tilde{\rho}^2}{5}+\frac{11416\tilde{\rho}^3}{5}+\frac{13552\tilde{\rho}^4}{3}$$
$$+\frac{11416\tilde{\rho}^5}{5}+\frac{1164\tilde{\rho}^6}{5}+\frac{8\tilde{\rho}^7}{35}+\frac{9\tilde{\rho}^8}{70}+32\tilde{\rho}^{3/2}+\frac{14944}{15}\tilde{\rho}^{5/2}+\frac{141504}{35}\tilde{\rho}^{7/2}+\frac{141504}{35}\tilde{\rho}^{9/2}$$
$$+\frac{14944}{15}\tilde{\rho}^{11/2}+32\tilde{\rho}^{13/2}\Big)\Big\}. \tag{B.5}$$

The analytic results for power-suppressed contributions $Q^{(0)}_{i,0,\mu_G}$, $Q^{(1)}_{i,0,\mu_G}$ and $Q^{(1)}_{i,0,\rho_{LS}}$ are given by

$$Q^{(0)}_{0,0,\mu_G}=-\frac{5\tilde{\rho}^4}{2}+12\tilde{\rho}^3-12\tilde{\rho}^2-6\tilde{\rho}^2\ln(\tilde{\rho})+4\tilde{\rho}-\frac{3}{2}, \tag{B.6}$$

$$Q^{(0)}_{1,0,\mu_G}=\tilde{\rho}\Big(-9\tilde{\rho}^2+3\tilde{\rho}-4\Big)\ln(\tilde{\rho})+\frac{1}{12}\Big(-9\tilde{\rho}^5+79\tilde{\rho}^4-48\tilde{\rho}^3-7\tilde{\rho}-15\Big), \tag{B.7}$$

$$Q^{(0)}_{2,0,\mu_G}=-\frac{1}{3}(\tilde{\rho}-1)^2\Big(\tilde{\rho}^4-12\tilde{\rho}^3-36\tilde{\rho}^2+44\tilde{\rho}+12(3\tilde{\rho}+2)\tilde{\rho}\ln(\tilde{\rho})+3\Big), \tag{B.8}$$

$$Q^{(0)}_{3,0,\mu_G}=\frac{1}{140}\Big(-25\tilde{\rho}^7+511\tilde{\rho}^6+1715\tilde{\rho}^5-18725\tilde{\rho}^4+11025\tilde{\rho}^3+9625\tilde{\rho}^2-4011\tilde{\rho}-115\Big)+$$
$$-3\tilde{\rho}\Big(5\tilde{\rho}^4-15\tilde{\rho}^3-35\tilde{\rho}^2+5\tilde{\rho}+4\Big)\ln(\tilde{\rho}), \tag{B.9}$$

$$Q^{(0)}_{4,0,\mu_G}=\frac{1}{420}\Big(-45\tilde{\rho}^8+1264\tilde{\rho}^7+9156\tilde{\rho}^6-140784\tilde{\rho}^5-81200\tilde{\rho}^4+216720\tilde{\rho}^3+15036\tilde{\rho}^2+$$
$$-19856\tilde{\rho}-291)-2\tilde{\rho}\Big(9\tilde{\rho}^5-48\tilde{\rho}^4-245\tilde{\rho}^3-120\tilde{\rho}^2+33\tilde{\rho}+8\Big)\ln(\tilde{\rho}), \tag{B.10}$$

$$Q^{(1)}_{0,0,\mu_G}=C_A\Big\{-\frac{1}{36}-\frac{3805\tilde{\rho}}{216}+\frac{2431\tilde{\rho}^2}{216}+\frac{415\tilde{\rho}^3}{72}+\frac{5\tilde{\rho}^4}{8}+\ln\left(1-\sqrt{\tilde{\rho}}\right)\Big[-\frac{5}{108}-\frac{5}{36\tilde{\rho}}$$
$$+2\tilde{\rho}+\frac{8\tilde{\rho}^2}{9}-\frac{265\tilde{\rho}^3}{108}-\frac{\tilde{\rho}^4}{4}+\ln(\tilde{\rho})\Big(-\frac{17}{9}+5\tilde{\rho}+\frac{5\tilde{\rho}^2}{3}+\frac{37\tilde{\rho}^3}{9}+\frac{16}{3}\sqrt{\tilde{\rho}}-\frac{176}{9}\tilde{\rho}^{3/2}\Big)\Big]$$
$$+\ln(\tilde{\rho})\Big[-\frac{131\tilde{\rho}}{18}-12\tilde{\rho}^2-\frac{131\tilde{\rho}^3}{108}+\frac{\tilde{\rho}^4}{4}+\ln(1-\tilde{\rho})(\frac{16}{9}-6\tilde{\rho}+\frac{26\tilde{\rho}^2}{3}-\frac{56\tilde{\rho}^3}{9}+$$
$$-\frac{8}{3}\sqrt{\tilde{\rho}}+\frac{88}{9}\tilde{\rho}^{3/2})\Big]+\ln\Big(\frac{\mu_s}{m_b}\Big)\Big(-\frac{3}{4}+2\tilde{\rho}-6\tilde{\rho}^2+6\tilde{\rho}^3-\frac{5\tilde{\rho}^4}{4}-3\tilde{\rho}^2\ln(\tilde{\rho})\Big)$$
$$+\ln\left(1+\sqrt{\tilde{\rho}}\right)\Big[-\frac{5}{108}-\frac{5}{36\tilde{\rho}}+2\tilde{\rho}+\frac{8\tilde{\rho}^2}{9}-\frac{265\tilde{\rho}^3}{108}-\frac{\tilde{\rho}^4}{4}+\Big(-\frac{17}{9}+5\tilde{\rho}+\frac{5\tilde{\rho}^2}{3}$$
$$+\frac{37\tilde{\rho}^3}{9}\Big)\ln(\tilde{\rho})\Big]+\pi^2\Big(-\frac{1}{18}+\frac{\tilde{\rho}}{3}-\frac{4\tilde{\rho}^2}{3}+\frac{11\tilde{\rho}^3}{18}-\frac{4}{3}\sqrt{\tilde{\rho}}+\frac{44}{9}\tilde{\rho}^{3/2}\Big)$$
$$+\mathrm{Li}_2(\tilde{\rho})\Big(\frac{1}{3}-2\tilde{\rho}+8\tilde{\rho}^2-\frac{11\tilde{\rho}^3}{3}-\frac{8}{3}\sqrt{\tilde{\rho}}+\frac{88}{9}\tilde{\rho}^{3/2}\Big)+\Big(\frac{\tilde{\rho}}{2}-\frac{11\tilde{\rho}^2}{6}+\frac{5\tilde{\rho}^3}{18}\Big)\ln^2(\tilde{\rho})$$
$$+\Big(\frac{32}{3}\sqrt{\tilde{\rho}}-\frac{352}{9}\tilde{\rho}^{3/2}\Big)\mathrm{Li}_2(\sqrt{\tilde{\rho}})\Big\}+C_F\Big\{-\frac{215}{144}+\frac{3733\tilde{\rho}}{108}-\frac{1360\tilde{\rho}^2}{27}+\frac{985\tilde{\rho}^3}{36}+$$
$$-\frac{161\tilde{\rho}^4}{16}+\ln(\tilde{\rho})\Big[\frac{125\tilde{\rho}}{9}-\frac{109\tilde{\rho}^2}{18}+\frac{667\tilde{\rho}^3}{27}-\frac{65\tilde{\rho}^4}{12}+\ln(1-\tilde{\rho})\Big(-\frac{14}{9}+24\tilde{\rho}+$$

JHEP08(2022)039

$$-\frac{74\tilde{\rho}^2}{3}-\frac{152\tilde{\rho}^3}{9}+10\tilde{\rho}^4+\frac{32}{3}\sqrt{\tilde{\rho}}-\frac{128}{9}\tilde{\rho}^{3/2}\Big)\Big]+\ln\left(1-\sqrt{\tilde{\rho}}\right)\Big[\frac{31}{108}-\frac{1}{9\tilde{\rho}}-\frac{26\tilde{\rho}}{3}$$
$$+\frac{226\tilde{\rho}^2}{9}-\frac{595\tilde{\rho}^3}{27}+\frac{65\tilde{\rho}^4}{12}+\ln(\tilde{\rho})\Big(\frac{25}{9}-18\tilde{\rho}+\frac{58\tilde{\rho}^2}{3}+\frac{58\tilde{\rho}^3}{9}-5\tilde{\rho}^4-\frac{64}{3}\sqrt{\tilde{\rho}}$$
$$+\frac{256}{9}\tilde{\rho}^{3/2}\Big)\Big]+\ln\left(1+\sqrt{\tilde{\rho}}\right)\Big[\frac{31}{108}-\frac{1}{9\tilde{\rho}}-\frac{26\tilde{\rho}}{3}+\frac{226\tilde{\rho}^2}{9}-\frac{595\tilde{\rho}^3}{27}+\frac{65\tilde{\rho}^4}{12}$$
$$+\Big(\frac{25}{9}-18\tilde{\rho}+\frac{58\tilde{\rho}^2}{3}+\frac{58\tilde{\rho}^3}{9}-5\tilde{\rho}^4\Big)\ln(\tilde{\rho})\Big]+\mathrm{Li}_2(\tilde{\rho})\Big(\frac{5}{6}+12\tilde{\rho}-12\tilde{\rho}^2+$$
$$-\frac{44\tilde{\rho}^3}{3}+\frac{15\tilde{\rho}^4}{2}+\frac{32}{3}\sqrt{\tilde{\rho}}-\frac{128}{9}\tilde{\rho}^{3/2}\Big)+\pi^2\Big(-\frac{5}{36}-2\tilde{\rho}+2\tilde{\rho}^2+\frac{22\tilde{\rho}^3}{9}-\frac{5\tilde{\rho}^4}{4}$$
$$+\frac{16}{3}\sqrt{\tilde{\rho}}-\frac{64}{9}\tilde{\rho}^{3/2}\Big)+\Big(-2\tilde{\rho}-\frac{5\tilde{\rho}^2}{3}+\frac{28\tilde{\rho}^3}{9}-\frac{5\tilde{\rho}^4}{4}\Big)\ln^2(\tilde{\rho})$$
$$+\Big(-\frac{128}{3}\sqrt{\tilde{\rho}}+\frac{512}{9}\tilde{\rho}^{3/2}\Big)\mathrm{Li}_2(\sqrt{\tilde{\rho}})\Big\},\tag{B.11}$$

$$Q^{(1)}_{1,0,\mu_G}=C_A\Big\{\frac{139}{180}-\frac{29779\tilde{\rho}}{2160}-\frac{8398\tilde{\rho}^2}{135}+\frac{74623\tilde{\rho}^3}{1080}+\frac{1069\tilde{\rho}^4}{180}+\frac{3\tilde{\rho}^5}{16}$$
$$+\ln\left(1-\sqrt{\tilde{\rho}}\right)\Big[-\frac{67}{540}-\frac{17}{360\tilde{\rho}}+\frac{1453\tilde{\rho}}{216}+\frac{11\tilde{\rho}^2}{9}-\frac{1145\tilde{\rho}^3}{216}-\frac{1297\tilde{\rho}^4}{540}-\frac{3\tilde{\rho}^5}{40}$$
$$+\ln(\tilde{\rho})\Big(-\frac{5}{9}+\frac{47\tilde{\rho}}{9}+\frac{50\tilde{\rho}^2}{3}+\frac{91\tilde{\rho}^3}{9}+\frac{17\tilde{\rho}^4}{9}+\frac{16}{3}\sqrt{\tilde{\rho}}+\frac{64}{9}\tilde{\rho}^{3/2}-\frac{880}{9}\tilde{\rho}^{5/2}\Big)\Big]$$
$$+\ln(\tilde{\rho})\Big[\frac{29\tilde{\rho}}{36}-\frac{383\tilde{\rho}^2}{9}-\frac{7723\tilde{\rho}^3}{216}+\frac{43\tilde{\rho}^4}{135}+\frac{3\tilde{\rho}^5}{40}+\ln(1-\tilde{\rho})\Big(\frac{10}{9}-\frac{157\tilde{\rho}}{9}+\frac{50\tilde{\rho}^2}{3}$$
$$+\frac{115\tilde{\rho}^3}{9}-\frac{34\tilde{\rho}^4}{9}-\frac{8}{3}\sqrt{\tilde{\rho}}-\frac{32}{9}\tilde{\rho}^{3/2}+\frac{440}{9}\tilde{\rho}^{5/2}\Big)\Big]+\ln\Big(\frac{\mu_s}{m_b}\Big)\Big[-\frac{5}{8}-\frac{7\tilde{\rho}}{24}-2\tilde{\rho}^3$$
$$+\frac{79\tilde{\rho}^4}{24}-\frac{3\tilde{\rho}^5}{8}+\Big(-2\tilde{\rho}+\frac{3\tilde{\rho}^2}{2}-\frac{9\tilde{\rho}^3}{2}\Big)\ln(\tilde{\rho})\Big]+\ln\left(1+\sqrt{\tilde{\rho}}\right)\Big[-\frac{67}{540}-\frac{17}{360\tilde{\rho}}$$
$$+\frac{1453\tilde{\rho}}{216}+\frac{11\tilde{\rho}^2}{9}-\frac{1145\tilde{\rho}^3}{216}-\frac{1297\tilde{\rho}^4}{540}-\frac{3\tilde{\rho}^5}{40}+\Big(-\frac{5}{9}+\frac{47\tilde{\rho}}{9}+\frac{50\tilde{\rho}^2}{3}+\frac{91\tilde{\rho}^3}{9}$$
$$+\frac{17\tilde{\rho}^4}{9}\Big)\ln(\tilde{\rho})\Big]+\pi^2\Big(-\frac{5}{36}+\frac{89\tilde{\rho}}{36}-\frac{25\tilde{\rho}^2}{6}-\frac{107\tilde{\rho}^3}{36}+\frac{17\tilde{\rho}^4}{36}-\frac{4}{3}\sqrt{\tilde{\rho}}-\frac{16}{9}\tilde{\rho}^{3/2}$$
$$+\frac{220}{9}\tilde{\rho}^{5/2}\Big)+\mathrm{Li}_2(\tilde{\rho})\Big(\frac{5}{6}-\frac{89\tilde{\rho}}{6}+25\tilde{\rho}^2+\frac{107\tilde{\rho}^3}{6}-\frac{17\tilde{\rho}^4}{6}-\frac{8}{3}\sqrt{\tilde{\rho}}-\frac{32}{9}\tilde{\rho}^{3/2}$$
$$+\frac{440}{9}\tilde{\rho}^{5/2}\Big)+\Big(\frac{11\tilde{\rho}}{4}-\frac{16\tilde{\rho}^2}{3}-\frac{103\tilde{\rho}^3}{18}+\frac{17\tilde{\rho}^4}{36}\Big)\ln^2(\tilde{\rho})+\Big(\frac{32}{3}\sqrt{\tilde{\rho}}+\frac{128}{9}\tilde{\rho}^{3/2}+$$
$$-\frac{1760}{9}\tilde{\rho}^{5/2}\Big)\mathrm{Li}_2(\sqrt{\tilde{\rho}})\Big\}+C_F\Big\{-\frac{2771}{720}+\frac{75529\tilde{\rho}}{2160}+\frac{70027\tilde{\rho}^2}{1080}-\frac{7597\tilde{\rho}^3}{72}+\frac{9121\tilde{\rho}^4}{720}+$$

JHEP08(2022)039

$$
\begin{aligned}
&-\frac{249\tilde{\rho}^5}{80}+\ln(\tilde{\rho})\Big[-\frac{91\tilde{\rho}}{72}+\frac{317\tilde{\rho}^2}{4}+\frac{3815\tilde{\rho}^3}{108}+\frac{2527\tilde{\rho}^4}{180}-\frac{241\tilde{\rho}^5}{120}+\ln(1-\tilde{\rho})\Big(-\frac{13}{9}\\
&+\frac{109\tilde{\rho}}{3}-\frac{197\tilde{\rho}^2}{3}-\frac{463\tilde{\rho}^3}{9}-9\tilde{\rho}^4+3\tilde{\rho}^5+\frac{32}{3}\sqrt{\tilde{\rho}}+\frac{32}{9}\tilde{\rho}^{3/2}-\frac{256}{3}\tilde{\rho}^{5/2}\Big)\Big]\\
&+\ln\left(1-\sqrt{\tilde{\rho}}\right)\Big[\frac{1511}{1080}-\frac{2}{45\tilde{\rho}}-\frac{623\tilde{\rho}}{72}+\frac{109\tilde{\rho}^2}{9}+\frac{187\tilde{\rho}^3}{27}-\frac{4949\tilde{\rho}^4}{360}+\frac{241\tilde{\rho}^5}{120}\\
&+\ln(\tilde{\rho})\Big(\frac{13}{18}-\frac{13\tilde{\rho}}{6}-\frac{38\tilde{\rho}^2}{3}+\frac{254\tilde{\rho}^3}{9}+\frac{9\tilde{\rho}^4}{2}-\frac{3\tilde{\rho}^5}{2}-\frac{64}{3}\sqrt{\tilde{\rho}}-\frac{64}{9}\tilde{\rho}^{3/2}+\frac{512}{3}\tilde{\rho}^{5/2}\Big)\Big]\\
&+\ln\left(1+\sqrt{\tilde{\rho}}\right)\Big[\frac{1511}{1080}-\frac{2}{45\tilde{\rho}}-\frac{623\tilde{\rho}}{72}+\frac{109\tilde{\rho}^2}{9}+\frac{187\tilde{\rho}^3}{27}-\frac{4949\tilde{\rho}^4}{360}+\frac{241\tilde{\rho}^5}{120}+\Big(\frac{13}{18}+\\
&-\frac{13\tilde{\rho}}{6}-\frac{38\tilde{\rho}^2}{3}+\frac{254\tilde{\rho}^3}{9}+\frac{9\tilde{\rho}^4}{2}-\frac{3\tilde{\rho}^5}{2}\Big)\ln(\tilde{\rho})\Big]+\mathrm{Li}_2(\tilde{\rho})\Big(-\frac{13}{12}+\frac{141\tilde{\rho}}{4}-72\tilde{\rho}^2+\\
&-\frac{112\tilde{\rho}^3}{3}-\frac{27\tilde{\rho}^4}{4}+\frac{9\tilde{\rho}^5}{4}+\frac{32}{3}\sqrt{\tilde{\rho}}+\frac{32}{9}\tilde{\rho}^{3/2}-\frac{256}{3}\tilde{\rho}^{5/2}\Big)+\pi^2\Big(\frac{13}{72}-\frac{47\tilde{\rho}}{8}+12\tilde{\rho}^2\\
&+\frac{56\tilde{\rho}^3}{9}+\frac{9\tilde{\rho}^4}{8}-\frac{3\tilde{\rho}^5}{8}+\frac{16}{3}\sqrt{\tilde{\rho}}+\frac{16}{9}\tilde{\rho}^{3/2}-\frac{128}{3}\tilde{\rho}^{5/2}\Big)+\Big(-7\tilde{\rho}+\frac{83\tilde{\rho}^2}{6}+\frac{37\tilde{\rho}^3}{18}\\
&+\frac{9\tilde{\rho}^4}{8}-\frac{3\tilde{\rho}^5}{8}\Big)\ln^2(\tilde{\rho})+\Big(-\frac{128}{3}\sqrt{\tilde{\rho}}-\frac{128}{9}\tilde{\rho}^{3/2}+\frac{1024}{3}\tilde{\rho}^{5/2}\Big)\mathrm{Li}_2(\sqrt{\tilde{\rho}})\Big\},
\end{aligned}
\tag{B.12}
$$

$$
\begin{aligned}
Q^{(1)}_{2,0,\mu_G}=C_F\Big\{&-\frac{293}{90}-\frac{237923\tilde{\rho}}{5400}+\frac{362632\tilde{\rho}^2}{675}-\frac{417839\tilde{\rho}^3}{1350}-\frac{127349\tilde{\rho}^4}{675}+\frac{10451\tilde{\rho}^5}{1080}+\\
&-\frac{383\tilde{\rho}^6}{270}+\ln^2(\tilde{\rho})\Big(-12\tilde{\rho}+\frac{29\tilde{\rho}^2}{3}+\frac{833\tilde{\rho}^3}{9}+\frac{20\tilde{\rho}^4}{9}+\frac{37\tilde{\rho}^5}{45}-\frac{\tilde{\rho}^6}{6}\Big)\\
&+\ln\left(1+\sqrt{\tilde{\rho}}\right)\Big[\frac{2053}{1350}-\frac{1}{45\tilde{\rho}}-\frac{338\tilde{\rho}}{135}-\frac{550\tilde{\rho}^2}{27}+\frac{1135\tilde{\rho}^3}{27}-\frac{2969\tilde{\rho}^4}{270}-\frac{7214\tilde{\rho}^5}{675}\\
&+\frac{46\tilde{\rho}^6}{45}+\ln(\tilde{\rho})\Big(\frac{28}{45}+\frac{44\tilde{\rho}}{9}-\frac{250\tilde{\rho}^2}{9}-\frac{40\tilde{\rho}^3}{9}+\frac{368\tilde{\rho}^4}{9}+\frac{148\tilde{\rho}^5}{45}-\frac{2\tilde{\rho}^6}{3}\Big)\Big]\\
&+\ln(\tilde{\rho})\Big[-\frac{1573\tilde{\rho}}{45}+\frac{17197\tilde{\rho}^2}{90}+\frac{51568\tilde{\rho}^3}{135}+\frac{19901\tilde{\rho}^4}{270}+\frac{14203\tilde{\rho}^5}{1350}-\frac{46\tilde{\rho}^6}{45}\\
&+\ln(1-\tilde{\rho})\Big(-\frac{56}{45}+\frac{488\tilde{\rho}}{9}-\frac{520\tilde{\rho}^2}{9}-\frac{3544\tilde{\rho}^3}{9}-\frac{664\tilde{\rho}^4}{9}-\frac{296\tilde{\rho}^5}{45}+\frac{4\tilde{\rho}^6}{3}+\frac{32}{3}\sqrt{\tilde{\rho}}\\
&+\frac{704}{9}\tilde{\rho}^{3/2}-\frac{15776}{45}\tilde{\rho}^{5/2}-\frac{1792}{9}\tilde{\rho}^{7/2}\Big)\Big]+\ln\left(1-\sqrt{\tilde{\rho}}\right)\Big[\frac{2053}{1350}-\frac{1}{45\tilde{\rho}}-\frac{338\tilde{\rho}}{135}+\\
&-\frac{550\tilde{\rho}^2}{27}+\frac{1135\tilde{\rho}^3}{27}-\frac{2969\tilde{\rho}^4}{270}-\frac{7214\tilde{\rho}^5}{675}+\frac{46\tilde{\rho}^6}{45}+\ln(\tilde{\rho})\Big(\frac{28}{45}+\frac{44\tilde{\rho}}{9}-\frac{250\tilde{\rho}^2}{9}+\\
&-\frac{40\tilde{\rho}^3}{9}+\frac{368\tilde{\rho}^4}{9}+\frac{148\tilde{\rho}^5}{45}-\frac{2\tilde{\rho}^6}{3}-\frac{64}{3}\sqrt{\tilde{\rho}}-\frac{1408}{9}\tilde{\rho}^{3/2}+\frac{31552}{45}\tilde{\rho}^{5/2}+\frac{3584}{9}\tilde{\rho}^{7/2}\Big)\Big]
\end{aligned}
$$

JHEP08(2022)039

$$+\mathrm{Li}_2(\tilde{\rho})\Big(-\frac{14}{15}+\frac{170\tilde{\rho}}{3}-\frac{215\tilde{\rho}^2}{3}-396\tilde{\rho}^3-\frac{160\tilde{\rho}^4}{3}-\frac{74\tilde{\rho}^5}{15}+\tilde{\rho}^6+\frac{32}{3}\sqrt{\tilde{\rho}}+\frac{704}{9}\tilde{\rho}^{3/2}+$$
$$-\frac{15776}{45}\tilde{\rho}^{5/2}-\frac{1792}{9}\tilde{\rho}^{7/2}\Big)+\pi^2\Big(\frac{7}{45}-\frac{85\tilde{\rho}}{9}+\frac{215\tilde{\rho}^2}{18}+66\tilde{\rho}^3+\frac{80\tilde{\rho}^4}{9}+\frac{37\tilde{\rho}^5}{45}-\frac{\tilde{\rho}^6}{6}$$
$$+\frac{16}{3}\sqrt{\tilde{\rho}}+\frac{352}{9}\tilde{\rho}^{3/2}-\frac{7888}{45}\tilde{\rho}^{5/2}-\frac{896}{9}\tilde{\rho}^{7/2}\Big)+\mathrm{Li}_2(\sqrt{\tilde{\rho}})\Big(-\frac{128}{3}\sqrt{\tilde{\rho}}-\frac{2816}{9}\tilde{\rho}^{3/2}$$
$$+\frac{63104}{45}\tilde{\rho}^{5/2}+\frac{7168}{9}\tilde{\rho}^{7/2}\Big)\Big\}+C_A\Big\{\frac{683}{1800}+\frac{22571\tilde{\rho}}{2700}-\frac{322361\tilde{\rho}^2}{1350}+\frac{161147\tilde{\rho}^3}{2700}$$
$$+\frac{297611\tilde{\rho}^4}{1800}+\frac{247\tilde{\rho}^5}{50}+\frac{\tilde{\rho}^6}{12}+\ln\left(1-\sqrt{\tilde{\rho}}\right)\Big[-\frac{319}{2700}-\frac{1}{45\tilde{\rho}}+\frac{6143\tilde{\rho}}{540}+\frac{295\tilde{\rho}^2}{18}+$$
$$-\frac{365\tilde{\rho}^3}{27}-\frac{6413\tilde{\rho}^4}{540}-\frac{659\tilde{\rho}^5}{300}-\frac{\tilde{\rho}^6}{30}+\ln(\tilde{\rho})\Big(-\frac{17}{45}+\frac{67\tilde{\rho}}{9}+\frac{128\tilde{\rho}^2}{3}+\frac{404\tilde{\rho}^3}{9}+\frac{127\tilde{\rho}^4}{9}$$
$$+\frac{7\tilde{\rho}^5}{5}+\frac{16}{3}\sqrt{\tilde{\rho}}+\frac{560}{9}\tilde{\rho}^{3/2}-\frac{12208}{45}\tilde{\rho}^{5/2}-240\tilde{\rho}^{7/2}\Big)\Big]+\ln(\tilde{\rho})\Big[\frac{572\tilde{\rho}}{45}-\frac{7133\tilde{\rho}^2}{90}+$$
$$-\frac{56689\tilde{\rho}^3}{270}-\frac{8857\tilde{\rho}^4}{135}+\frac{56\tilde{\rho}^5}{75}+\frac{\tilde{\rho}^6}{30}+\ln(1-\tilde{\rho})\Big(\frac{34}{45}-\frac{242\tilde{\rho}}{9}-\frac{58\tilde{\rho}^2}{3}+\frac{1262\tilde{\rho}^3}{9}$$
$$+\frac{178\tilde{\rho}^4}{9}-\frac{14\tilde{\rho}^5}{5}-\frac{8}{3}\sqrt{\tilde{\rho}}-\frac{280}{9}\tilde{\rho}^{3/2}+\frac{6104}{45}\tilde{\rho}^{5/2}+120\tilde{\rho}^{7/2}\Big)\Big]$$
$$+\ln\left(\frac{\mu_s}{m_b}\right)\Big[-\frac{1}{2}-\frac{19\tilde{\rho}}{3}+\frac{121\tilde{\rho}^2}{6}-\frac{52\tilde{\rho}^3}{3}+\frac{11\tilde{\rho}^4}{6}+\frac{7\tilde{\rho}^5}{3}-\frac{\tilde{\rho}^6}{6}+\Big(-4\tilde{\rho}+2\tilde{\rho}^2$$
$$+8\tilde{\rho}^3-6\tilde{\rho}^4\Big)\ln(\tilde{\rho})\Big]+\ln\left(1+\sqrt{\tilde{\rho}}\right)\Big[-\frac{319}{2700}-\frac{1}{45\tilde{\rho}}+\frac{6143\tilde{\rho}}{540}+\frac{295\tilde{\rho}^2}{18}-\frac{365\tilde{\rho}^3}{27}+$$
$$-\frac{6413\tilde{\rho}^4}{540}-\frac{659\tilde{\rho}^5}{300}-\frac{\tilde{\rho}^6}{30}+\Big(-\frac{17}{45}+\frac{67\tilde{\rho}}{9}+\frac{128\tilde{\rho}^2}{3}+\frac{404\tilde{\rho}^3}{9}+\frac{127\tilde{\rho}^4}{9}+\frac{7\tilde{\rho}^5}{5}\Big)\ln(\tilde{\rho})\Big)$$
$$+\mathrm{Li}_2(\sqrt{\tilde{\rho}})\Big(\frac{32}{3}\sqrt{\tilde{\rho}}+\frac{1120}{9}\tilde{\rho}^{3/2}-\frac{24416}{45}\tilde{\rho}^{5/2}-480\tilde{\rho}^{7/2}\Big)+\pi^2\Big(-\frac{17}{180}+\frac{139\tilde{\rho}}{36}-\frac{\tilde{\rho}^2}{3}+$$
$$-\frac{244\tilde{\rho}^3}{9}-\frac{161\tilde{\rho}^4}{36}+\frac{7\tilde{\rho}^5}{20}-\frac{4}{3}\sqrt{\tilde{\rho}}-\frac{140}{9}\tilde{\rho}^{3/2}+\frac{3052}{45}\tilde{\rho}^{5/2}+60\tilde{\rho}^{7/2}\Big)+\mathrm{Li}_2(\tilde{\rho})\Big(\frac{17}{30}+$$
$$-\frac{139\tilde{\rho}}{6}+2\tilde{\rho}^2+\frac{488\tilde{\rho}^3}{3}+\frac{161\tilde{\rho}^4}{6}-\frac{21\tilde{\rho}^5}{10}-\frac{8}{3}\sqrt{\tilde{\rho}}-\frac{280}{9}\tilde{\rho}^{3/2}+\frac{6104}{45}\tilde{\rho}^{5/2}+120\tilde{\rho}^{7/2}\Big)$$
$$+\Big(5\tilde{\rho}+\frac{\tilde{\rho}^2}{6}-\frac{725\tilde{\rho}^3}{18}-\frac{305\tilde{\rho}^4}{36}+\frac{7\tilde{\rho}^5}{20}\Big)\ln^2(\tilde{\rho})\Big\}, \tag{B.13}$$

$$Q^{(1)}_{3,0,\mu_G}=C_A\Big\{\frac{1147}{6480}+\frac{990487\tilde{\rho}}{25200}-\frac{32728597\tilde{\rho}^2}{75600}-\frac{16174537\tilde{\rho}^3}{25200}+\frac{6247889\tilde{\rho}^4}{8400}+\frac{21711847\tilde{\rho}^5}{75600}$$
$$+\frac{963427\tilde{\rho}^6}{226800}+\frac{5\tilde{\rho}^7}{112}+\ln^2(\tilde{\rho})\Big(\frac{29\tilde{\rho}}{4}+\frac{289\tilde{\rho}^2}{12}-\frac{3925\tilde{\rho}^3}{36}-\frac{967\tilde{\rho}^4}{8}-\frac{34\tilde{\rho}^5}{3}+\frac{101\tilde{\rho}^6}{360}\Big)$$

JHEP08(2022)039

$$+\ln\left(1+\sqrt{\tilde{\rho}}\right)\left[-\frac{263}{2520}-\frac{31}{2520\tilde{\rho}}+\frac{4849\tilde{\rho}}{300}+\frac{3997\tilde{\rho}^2}{72}-\frac{5\tilde{\rho}^3}{6}-\frac{5989\tilde{\rho}^4}{120}-\frac{3383\tilde{\rho}^5}{180}+\right.$$
$$-\frac{25283\tilde{\rho}^6}{12600}-\frac{\tilde{\rho}^7}{56}+\ln(\tilde{\rho})\left(-\frac{5}{18}+\frac{47\tilde{\rho}}{5}+\frac{515\tilde{\rho}^2}{6}+\frac{1430\tilde{\rho}^3}{9}+\frac{179\tilde{\rho}^4}{2}+\frac{53\tilde{\rho}^5}{3}\right.$$
$$\left.\left.+\frac{101\tilde{\rho}^6}{90}\right)\right]+\ln\left(1-\sqrt{\tilde{\rho}}\right)\left[-\frac{263}{2520}-\frac{31}{2520\tilde{\rho}}+\frac{4849\tilde{\rho}}{300}+\frac{3997\tilde{\rho}^2}{72}-\frac{5\tilde{\rho}^3}{6}-\frac{5989\tilde{\rho}^4}{120}+\right.$$
$$-\frac{3383\tilde{\rho}^5}{180}-\frac{25283\tilde{\rho}^6}{12600}-\frac{\tilde{\rho}^7}{56}+\ln(\tilde{\rho})\left(-\frac{5}{18}+\frac{47\tilde{\rho}}{5}+\frac{515\tilde{\rho}^2}{6}+\frac{1430\tilde{\rho}^3}{9}+\frac{179\tilde{\rho}^4}{2}\right.$$
$$\left.\left.+\frac{53\tilde{\rho}^5}{3}+\frac{101\tilde{\rho}^6}{90}+\frac{16}{3}\sqrt{\tilde{\rho}}+\frac{1312}{9}\tilde{\rho}^{3/2}-384\tilde{\rho}^{5/2}-\frac{7072}{5}\tilde{\rho}^{7/2}-\frac{4016}{9}\tilde{\rho}^{9/2}\right)\right]$$
$$+\ln(\tilde{\rho})\left[\frac{2473\tilde{\rho}}{90}-\frac{6971\tilde{\rho}^2}{90}-\frac{762761\tilde{\rho}^3}{1080}-\frac{7781\tilde{\rho}^4}{12}-\frac{9007\tilde{\rho}^5}{90}+\frac{5659\tilde{\rho}^6}{6300}+\frac{\tilde{\rho}^7}{56}\right.$$
$$+\ln(1-\tilde{\rho})\left(\frac{5}{9}-\frac{179\tilde{\rho}}{5}-\frac{394\tilde{\rho}^2}{3}+\frac{3526\tilde{\rho}^3}{9}+434\tilde{\rho}^4+\frac{83\tilde{\rho}^5}{3}-\frac{101\tilde{\rho}^6}{45}-\frac{8}{3}\sqrt{\tilde{\rho}}+\right.$$
$$\left.-\frac{656}{9}\tilde{\rho}^{3/2}+192\tilde{\rho}^{5/2}+\frac{3536}{5}\tilde{\rho}^{7/2}+\frac{2008}{9}\tilde{\rho}^{9/2}\right)\Big]+\ln\left(\frac{\mu_s}{m_b}\right)\left[-\frac{23}{56}-\frac{573\tilde{\rho}}{40}\right.$$
$$+\frac{275\tilde{\rho}^2}{8}+\frac{315\tilde{\rho}^3}{8}-\frac{535\tilde{\rho}^4}{8}+\frac{49\tilde{\rho}^5}{8}+\frac{73\tilde{\rho}^6}{40}-\frac{5\tilde{\rho}^7}{56}+\left(-6\tilde{\rho}-\frac{15\tilde{\rho}^2}{2}+\frac{105\tilde{\rho}^3}{2}\right.$$
$$\left.\left.+\frac{45\tilde{\rho}^4}{2}-\frac{15\tilde{\rho}^5}{2}\right)\ln(\tilde{\rho})\right]+\mathrm{Li}_2(\sqrt{\tilde{\rho}})\left(\frac{32}{3}\sqrt{\tilde{\rho}}+\frac{2624}{9}\tilde{\rho}^{3/2}-768\tilde{\rho}^{5/2}-\frac{14144}{5}\tilde{\rho}^{7/2}+\right.$$
$$\left.-\frac{8032}{9}\tilde{\rho}^{9/2}\right)+\pi^2\left(-\frac{5}{72}+\frac{311\tilde{\rho}}{60}+\frac{1061\tilde{\rho}^2}{72}-\frac{4241\tilde{\rho}^3}{54}-\frac{1915\tilde{\rho}^4}{24}-\frac{73\tilde{\rho}^5}{12}+\frac{101\tilde{\rho}^6}{360}+\right.$$
$$-\frac{4}{3}\sqrt{\tilde{\rho}}-\frac{328}{9}\tilde{\rho}^{3/2}+96\tilde{\rho}^{5/2}+\frac{1768}{5}\tilde{\rho}^{7/2}+\frac{1004}{9}\tilde{\rho}^{9/2}\Big)+\mathrm{Li}_2(\tilde{\rho})\left(\frac{5}{12}-\frac{311\tilde{\rho}}{10}+\right.$$
$$-\frac{1061\tilde{\rho}^2}{12}+\frac{4241\tilde{\rho}^3}{9}+\frac{1915\tilde{\rho}^4}{4}+\frac{73\tilde{\rho}^5}{2}-\frac{101\tilde{\rho}^6}{60}-\frac{8}{3}\sqrt{\tilde{\rho}}-\frac{656}{9}\tilde{\rho}^{3/2}+192\tilde{\rho}^{5/2}$$
$$\left.\left.+\frac{3536}{5}\tilde{\rho}^{7/2}+\frac{2008}{9}\tilde{\rho}^{9/2}\right)\right\}+C_F\left\{-\frac{182927}{64800}-\frac{61448201\tilde{\rho}}{352800}+\frac{1126861973\tilde{\rho}^2}{1058400}\right.$$
$$+\frac{1267432219\tilde{\rho}^3}{1058400}-\frac{639220273\tilde{\rho}^4}{352800}-\frac{297234797\tilde{\rho}^5}{1058400}+\frac{26269529\tilde{\rho}^6}{3175200}-\frac{1567\tilde{\rho}^7}{2016}$$
$$+\ln^2(\tilde{\rho})\left(-17\tilde{\rho}-\frac{221\tilde{\rho}^2}{6}+\frac{3008\tilde{\rho}^3}{9}+\frac{2141\tilde{\rho}^4}{8}+\frac{53\tilde{\rho}^5}{24}+\frac{239\tilde{\rho}^6}{360}-\frac{5\tilde{\rho}^7}{56}\right)$$
$$+\ln\left(1+\sqrt{\tilde{\rho}}\right)\left[\frac{8597}{5880}-\frac{4}{315\tilde{\rho}}+\frac{3767\tilde{\rho}}{600}-\frac{3907\tilde{\rho}^2}{72}+\frac{475\tilde{\rho}^3}{72}+\frac{9467\tilde{\rho}^4}{120}-\frac{11009\tilde{\rho}^5}{360}+\right.$$
$$-\frac{113107\tilde{\rho}^6}{12600}+\frac{237\tilde{\rho}^7}{392}+\ln(\tilde{\rho})\left(\frac{67}{126}+\frac{111\tilde{\rho}}{10}-\frac{155\tilde{\rho}^2}{6}-\frac{2135\tilde{\rho}^3}{18}+\frac{33\tilde{\rho}^4}{2}+\frac{317\tilde{\rho}^5}{6}\right.$$
$$\left.\left.+\frac{239\tilde{\rho}^6}{90}-\frac{5\tilde{\rho}^7}{14}\right)\right]+\ln(\tilde{\rho})\left[-\frac{40357\tilde{\rho}}{504}+\frac{473153\tilde{\rho}^2}{2520}+\frac{1549664\tilde{\rho}^3}{945}+\frac{974059\tilde{\rho}^4}{840}\right.$$

JHEP08(2022)039

$$+\frac{23911\tilde{\rho}^5}{210}+\frac{7823\tilde{\rho}^6}{900}-\frac{237\tilde{\rho}^7}{392}+\ln(1-\tilde{\rho})\Big(-\frac{67}{63}+\frac{369\tilde{\rho}}{5}+\frac{340\tilde{\rho}^2}{3}-\frac{12404\tilde{\rho}^3}{9}+$$
$$-1092\tilde{\rho}^4-\frac{284\tilde{\rho}^5}{3}-\frac{239\tilde{\rho}^6}{45}+\frac{5\tilde{\rho}^7}{7}+\frac{32}{3}\sqrt{\tilde{\rho}}+\frac{1888}{9}\tilde{\rho}^{3/2}-608\tilde{\rho}^{5/2}-\frac{59552}{35}\tilde{\rho}^{7/2}+$$
$$-\frac{3200}{9}\tilde{\rho}^{9/2}\Big)\Big]+\ln\left(1-\sqrt{\tilde{\rho}}\right)\Big[\frac{8597}{5880}-\frac{4}{315\tilde{\rho}}+\frac{3767\tilde{\rho}}{600}-\frac{3907\tilde{\rho}^2}{72}+\frac{475\tilde{\rho}^3}{72}+\frac{9467\tilde{\rho}^4}{120}+$$
$$-\frac{11009\tilde{\rho}^5}{360}-\frac{113107\tilde{\rho}^6}{12600}+\frac{237\tilde{\rho}^7}{392}+\ln(\tilde{\rho})\Big(\frac{67}{126}+\frac{111\tilde{\rho}}{10}-\frac{155\tilde{\rho}^2}{6}-\frac{2135\tilde{\rho}^3}{18}+\frac{33\tilde{\rho}^4}{2}$$
$$+\frac{317\tilde{\rho}^5}{6}+\frac{239\tilde{\rho}^6}{90}-\frac{5\tilde{\rho}^7}{14}-\frac{64}{3}\sqrt{\tilde{\rho}}-\frac{3776}{9}\tilde{\rho}^{3/2}+1216\tilde{\rho}^{5/2}+\frac{119104}{35}\tilde{\rho}^{7/2}$$
$$+\frac{6400}{9}\tilde{\rho}^{9/2}\Big)\Big]+\mathrm{Li}_2(\tilde{\rho})\Big(-\frac{67}{84}+\frac{1587\tilde{\rho}}{20}+\frac{1205\tilde{\rho}^2}{12}-\frac{51751\tilde{\rho}^3}{36}-\frac{4335\tilde{\rho}^4}{4}-\frac{273\tilde{\rho}^5}{4}+$$
$$-\frac{239\tilde{\rho}^6}{60}+\frac{15\tilde{\rho}^7}{28}+\frac{32}{3}\sqrt{\tilde{\rho}}+\frac{1888}{9}\tilde{\rho}^{3/2}-608\tilde{\rho}^{5/2}-\frac{59552}{35}\tilde{\rho}^{7/2}-\frac{3200}{9}\tilde{\rho}^{9/2}\Big)$$
$$+\pi^2\Big(\frac{67}{504}-\frac{529\tilde{\rho}}{40}-\frac{1205\tilde{\rho}^2}{72}+\frac{51751\tilde{\rho}^3}{216}+\frac{1445\tilde{\rho}^4}{8}+\frac{91\tilde{\rho}^5}{8}+\frac{239\tilde{\rho}^6}{360}-\frac{5\tilde{\rho}^7}{56}$$
$$+\frac{16}{3}\sqrt{\tilde{\rho}}+\frac{944}{9}\tilde{\rho}^{3/2}-304\tilde{\rho}^{5/2}-\frac{29776}{35}\tilde{\rho}^{7/2}-\frac{1600}{9}\tilde{\rho}^{9/2}\Big)+\mathrm{Li}_2\left(\sqrt{\tilde{\rho}}\right)\Big(-\frac{128}{3}\sqrt{\tilde{\rho}}+$$
$$-\frac{7552}{9}\tilde{\rho}^{3/2}+2432\tilde{\rho}^{5/2}+\frac{238208}{35}\tilde{\rho}^{7/2}+\frac{12800}{9}\tilde{\rho}^{9/2}\Big)\Big\}, \tag{B.14}$$

$$Q^{(1)}_{4,0,\mu_G}=C_A\Big\{\frac{196879}{3175200}+\frac{24556379\tilde{\rho}}{317520}-\frac{274033471\tilde{\rho}^2}{529200}-\frac{3087900503\tilde{\rho}^3}{1058400}+\frac{17682109\tilde{\rho}^4}{42336}$$
$$+\frac{1326250231\tilde{\rho}^5}{529200}+\frac{683258473\tilde{\rho}^6}{1587600}+\frac{11880109\tilde{\rho}^7}{3175200}+\frac{3\tilde{\rho}^8}{112}+\ln^2(\tilde{\rho})\Big(\frac{19\tilde{\rho}}{2}+\frac{455\tilde{\rho}^2}{6}+$$
$$-\frac{1468\tilde{\rho}^3}{9}-\frac{10741\tilde{\rho}^4}{18}-\frac{3977\tilde{\rho}^5}{15}-\frac{641\tilde{\rho}^6}{45}+\frac{74\tilde{\rho}^7}{315}\Big)+\ln\left(1+\sqrt{\tilde{\rho}}\right)\Big[-\frac{2701}{29400}+$$
$$-\frac{19}{2520\tilde{\rho}}+\frac{66539\tilde{\rho}}{3150}+\frac{57841\tilde{\rho}^2}{450}+\frac{4942\tilde{\rho}^3}{45}-\frac{5201\tilde{\rho}^4}{45}-\frac{52157\tilde{\rho}^5}{450}-\frac{82039\tilde{\rho}^6}{3150}+$$
$$-\frac{18079\tilde{\rho}^7}{9800}-\frac{3\tilde{\rho}^8}{280}+\ln(\tilde{\rho})\Big(-\frac{68}{315}+\frac{506\tilde{\rho}}{45}+\frac{2246\tilde{\rho}^2}{15}+\frac{3974\tilde{\rho}^3}{9}+\frac{3862\tilde{\rho}^4}{9}$$
$$+\frac{2302\tilde{\rho}^5}{15}+\frac{946\tilde{\rho}^6}{45}+\frac{296\tilde{\rho}^7}{315}\Big)\Big]+\ln\left(1-\sqrt{\tilde{\rho}}\right)\Big[-\frac{2701}{29400}-\frac{19}{2520\tilde{\rho}}+\frac{66539\tilde{\rho}}{3150}$$
$$+\frac{57841\tilde{\rho}^2}{450}+\frac{4942\tilde{\rho}^3}{45}-\frac{5201\tilde{\rho}^4}{45}-\frac{52157\tilde{\rho}^5}{450}-\frac{82039\tilde{\rho}^6}{3150}-\frac{18079\tilde{\rho}^7}{9800}-\frac{3\tilde{\rho}^8}{280}$$
$$+\ln(\tilde{\rho})\Big(-\frac{68}{315}+\frac{506\tilde{\rho}}{45}+\frac{2246\tilde{\rho}^2}{15}+\frac{3974\tilde{\rho}^3}{9}+\frac{3862\tilde{\rho}^4}{9}+\frac{2302\tilde{\rho}^5}{15}+\frac{946\tilde{\rho}^6}{45}$$
$$+\frac{296\tilde{\rho}^7}{315}+\frac{16}{3}\sqrt{\tilde{\rho}}+\frac{2320}{9}\tilde{\rho}^{3/2}-\frac{8096}{45}\tilde{\rho}^{5/2}-\frac{154528}{35}\tilde{\rho}^{7/2}-\frac{194128}{45}\tilde{\rho}^{9/2}+$$

JHEP08(2022)039

$$-\frac{6448}{9}\tilde{\rho}^{11/2}\Big)\Big]+\ln(\tilde{\rho})\Big[\frac{13949\tilde{\rho}}{315}+\frac{524\tilde{\rho}^2}{21}-\frac{6215371\tilde{\rho}^3}{3780}-\frac{12309893\tilde{\rho}^4}{3780}+$$
$$-\frac{4810361\tilde{\rho}^5}{3150}-\frac{31034\tilde{\rho}^6}{225}+\frac{27917\tilde{\rho}^7}{29400}+\frac{3\tilde{\rho}^8}{280}+\ln(1-\tilde{\rho})\Big(\frac{136}{315}-\frac{2002\tilde{\rho}}{45}-\frac{5282\tilde{\rho}^2}{15}$$
$$+\frac{5266\tilde{\rho}^3}{9}+\frac{20558\tilde{\rho}^4}{9}+\frac{14506\tilde{\rho}^5}{15}+\frac{1618\tilde{\rho}^6}{45}-\frac{592\tilde{\rho}^7}{315}-\frac{8}{3}\sqrt{\tilde{\rho}}-\frac{1160}{9}\tilde{\rho}^{3/2}+\frac{4048}{45}\tilde{\rho}^{5/2}$$
$$+\frac{77264}{35}\tilde{\rho}^{7/2}+\frac{97064}{45}\tilde{\rho}^{9/2}+\frac{3224}{9}\tilde{\rho}^{11/2}\Big)\Big]+\ln\Big(\frac{\mu_s}{m_b}\Big)\Big[-\frac{97}{280}-\frac{2482\tilde{\rho}}{105}+\frac{179\tilde{\rho}^2}{10}$$
$$+258\tilde{\rho}^3-\frac{290\tilde{\rho}^4}{3}-\frac{838\tilde{\rho}^5}{5}+\frac{109\tilde{\rho}^6}{10}+\frac{158\tilde{\rho}^7}{105}-\frac{3\tilde{\rho}^8}{56}+\Big(-8\tilde{\rho}-33\tilde{\rho}^2+120\tilde{\rho}^3$$
$$+245\tilde{\rho}^4+48\tilde{\rho}^5-9\tilde{\rho}^6\Big)\ln(\tilde{\rho})\Big]+\mathrm{Li}_2(\sqrt{\tilde{\rho}})\Big(\frac{32}{3}\sqrt{\tilde{\rho}}+\frac{4640}{9}\tilde{\rho}^{3/2}-\frac{16192}{45}\tilde{\rho}^{5/2}+$$
$$-\frac{309056}{35}\tilde{\rho}^{7/2}-\frac{388256}{45}\tilde{\rho}^{9/2}-\frac{12896}{9}\tilde{\rho}^{11/2}\Big)+\pi^2\Big(-\frac{17}{315}+\frac{583\tilde{\rho}}{90}+\frac{4159\tilde{\rho}^2}{90}+$$
$$-\frac{7253\tilde{\rho}^3}{54}-\frac{22489\tilde{\rho}^4}{54}-\frac{5219\tilde{\rho}^5}{30}-\frac{697\tilde{\rho}^6}{90}+\frac{74\tilde{\rho}^7}{315}-\frac{4}{3}\sqrt{\tilde{\rho}}-\frac{580}{9}\tilde{\rho}^{3/2}+\frac{2024}{45}\tilde{\rho}^{5/2}$$
$$+\frac{38632}{35}\tilde{\rho}^{7/2}+\frac{48532}{45}\tilde{\rho}^{9/2}+\frac{1612}{9}\tilde{\rho}^{11/2}\Big)+\mathrm{Li}_2(\tilde{\rho})\Big(\frac{34}{105}-\frac{583\tilde{\rho}}{15}-\frac{4159\tilde{\rho}^2}{15}$$
$$+\frac{7253\tilde{\rho}^3}{9}+\frac{22489\tilde{\rho}^4}{9}+\frac{5219\tilde{\rho}^5}{5}+\frac{697\tilde{\rho}^6}{15}-\frac{148\tilde{\rho}^7}{105}-\frac{8}{3}\sqrt{\tilde{\rho}}-\frac{1160}{9}\tilde{\rho}^{3/2}+\frac{4048}{45}\tilde{\rho}^{5/2}$$
$$+\frac{77264}{35}\tilde{\rho}^{7/2}+\frac{97064}{45}\tilde{\rho}^{9/2}+\frac{3224}{9}\tilde{\rho}^{11/2}\Big)\Big\}+C_F\Big\{-\frac{6339713}{2540160}-\frac{26167927\tilde{\rho}}{75600}$$
$$+\frac{1186820717\tilde{\rho}^2}{1058400}+\frac{1265814329\tilde{\rho}^3}{176400}-\frac{584924819\tilde{\rho}^4}{264600}-\frac{2839397629\tilde{\rho}^5}{529200}+$$
$$-\frac{1204660967\tilde{\rho}^6}{3175200}+\frac{783799\tilde{\rho}^7}{105840}-\frac{44797\tilde{\rho}^8}{94080}+\ln^2(\tilde{\rho})\Big(-22\tilde{\rho}-\frac{445\tilde{\rho}^2}{3}+\frac{5962\tilde{\rho}^3}{9}$$
$$+\frac{3439\tilde{\rho}^4}{2}+\frac{8633\tilde{\rho}^5}{15}+\frac{19\tilde{\rho}^6}{9}+\frac{59\tilde{\rho}^7}{105}-\frac{3\tilde{\rho}^8}{56}\Big)+\ln\left(1+\sqrt{\tilde{\rho}}\right)\Big[\frac{240929}{176400}-\frac{1}{126\tilde{\rho}}$$
$$+\frac{36973\tilde{\rho}}{2205}-\frac{15911\tilde{\rho}^2}{225}-\frac{917\tilde{\rho}^3}{5}+\frac{1589\tilde{\rho}^4}{9}+\frac{26719\tilde{\rho}^5}{225}-\frac{16339\tilde{\rho}^6}{315}-\frac{172847\tilde{\rho}^7}{22050}$$
$$+\frac{4609\tilde{\rho}^8}{11760}+\ln(\tilde{\rho})\Big(\frac{289}{630}+\frac{356\tilde{\rho}}{21}+\frac{28\tilde{\rho}^2}{15}-\frac{2828\tilde{\rho}^3}{9}-350\tilde{\rho}^4+\frac{812\tilde{\rho}^5}{15}+\frac{580\tilde{\rho}^6}{9}$$
$$+\frac{236\tilde{\rho}^7}{105}-\frac{3\tilde{\rho}^8}{14}\Big)\Big]+\ln(\tilde{\rho})\Big[-\frac{83899\tilde{\rho}}{630}-\frac{79687\tilde{\rho}^2}{630}+\frac{7931981\tilde{\rho}^3}{1890}+\frac{1334683\tilde{\rho}^4}{180}$$
$$+\frac{8494769\tilde{\rho}^5}{3150}+\frac{19645\tilde{\rho}^6}{126}+\frac{83011\tilde{\rho}^7}{11025}-\frac{4609\tilde{\rho}^8}{11760}+\ln(1-\tilde{\rho})\Big(-\frac{289}{315}+\frac{1976\tilde{\rho}}{21}$$
$$+\frac{8354\tilde{\rho}^2}{15}-\frac{25816\tilde{\rho}^3}{9}-6679\tilde{\rho}^4-\frac{34384\tilde{\rho}^5}{15}-\frac{1034\tilde{\rho}^6}{9}-\frac{472\tilde{\rho}^7}{105}+\frac{3\tilde{\rho}^8}{7}+\frac{32}{3}\sqrt{\tilde{\rho}}$$

JHEP08(2022)039

$$+\frac{3584}{9}\tilde{\rho}^{3/2}-\frac{6464}{15}\tilde{\rho}^{5/2}-\frac{43648}{7}\tilde{\rho}^{7/2}-\frac{1581536}{315}\tilde{\rho}^{9/2}-\frac{1664}{3}\tilde{\rho}^{11/2}\Big)\Big]$$
$$+\ln\left(1-\sqrt{\tilde{\rho}}\right)\Big[\frac{240929}{176400}-\frac{1}{126\tilde{\rho}}+\frac{36973\tilde{\rho}}{2205}-\frac{15911\tilde{\rho}^2}{225}-\frac{917\tilde{\rho}^3}{5}+\frac{1589\tilde{\rho}^4}{9}$$
$$+\frac{26719\tilde{\rho}^5}{225}-\frac{16339\tilde{\rho}^6}{315}-\frac{172847\tilde{\rho}^7}{22050}+\frac{4609\tilde{\rho}^8}{11760}+\ln(\tilde{\rho})\Big(\frac{289}{630}+\frac{356\tilde{\rho}}{21}+\frac{28\tilde{\rho}^2}{15}+$$
$$-\frac{2828\tilde{\rho}^3}{9}-350\tilde{\rho}^4+\frac{812\tilde{\rho}^5}{15}+\frac{580\tilde{\rho}^6}{9}+\frac{236\tilde{\rho}^7}{105}-\frac{3\tilde{\rho}^8}{14}-\frac{64}{3}\sqrt{\tilde{\rho}}-\frac{7168}{9}\tilde{\rho}^{3/2}$$
$$+\frac{12928}{15}\tilde{\rho}^{5/2}+\frac{87296}{7}\tilde{\rho}^{7/2}+\frac{3163072}{315}\tilde{\rho}^{9/2}+\frac{3328}{3}\tilde{\rho}^{11/2}\Big)\Big]+\mathrm{Li}_2(\tilde{\rho})\Big(-\frac{289}{420}$$
$$+\frac{718\tilde{\rho}}{7}+\frac{8368\tilde{\rho}^2}{15}-\frac{27230\tilde{\rho}^3}{9}-6854\tilde{\rho}^4-\frac{11326\tilde{\rho}^5}{5}-\frac{248\tilde{\rho}^6}{3}-\frac{118\tilde{\rho}^7}{35}+\frac{9\tilde{\rho}^8}{28}$$
$$+\frac{32}{3}\sqrt{\tilde{\rho}}+\frac{3584}{9}\tilde{\rho}^{3/2}-\frac{6464}{15}\tilde{\rho}^{5/2}-\frac{43648}{7}\tilde{\rho}^{7/2}-\frac{1581536}{315}\tilde{\rho}^{9/2}-\frac{1664}{3}\tilde{\rho}^{11/2}\Big)$$
$$+\pi^2\Big(\frac{289}{2520}-\frac{359\tilde{\rho}}{21}-\frac{4184\tilde{\rho}^2}{45}+\frac{13615\tilde{\rho}^3}{27}+\frac{3427\tilde{\rho}^4}{3}+\frac{5663\tilde{\rho}^5}{15}+\frac{124\tilde{\rho}^6}{9}+\frac{59\tilde{\rho}^7}{105}+$$
$$-\frac{3\tilde{\rho}^8}{56}+\frac{16}{3}\sqrt{\tilde{\rho}}+\frac{1792}{9}\tilde{\rho}^{3/2}-\frac{3232}{15}\tilde{\rho}^{5/2}-\frac{21824}{7}\tilde{\rho}^{7/2}-\frac{790768}{315}\tilde{\rho}^{9/2}-\frac{832}{3}\tilde{\rho}^{11/2}\Big)$$
$$+\mathrm{Li}_2\left(\sqrt{\tilde{\rho}}\right)\Big(-\frac{128}{3}\sqrt{\tilde{\rho}}-\frac{14336}{9}\tilde{\rho}^{3/2}+\frac{25856}{15}\tilde{\rho}^{5/2}+\frac{174592}{7}\tilde{\rho}^{7/2}+\frac{6326144}{315}\tilde{\rho}^{9/2}$$
$$+\frac{6656}{3}\tilde{\rho}^{11/2}\Big)\Big\}, \tag{B.15}$$

$$Q^{(1)}_{i,0,\tilde{\rho}_{LS}}=-Q^{(1)}_{i,0,\mu_G}-\frac{1}{2}\left(C_A\ln\left(\frac{\mu_s}{m_b}\right)+C_A+C_F\right)Q^{(0)}_{i,0,\mu_G}, \tag{B.16}$$

where $\tilde{\rho}=m_c^2/m_b^2$. The results presented in this appendix are obtained from the differential expressions of ref. [15] after integration over the dilepton pair invariant mass squared.

The analytic expressions shown in the appendix can also be obtained from [35].

References

[1] HFLAV collaboration, *Averages of b-hadron, c-hadron, and τ-lepton properties as of 2018*, *Eur. Phys. J. C* **81** (2021) 226 [arXiv:1909.12524] [INSPIRE].

[2] A. Crivellin and S. Pokorski, *Can the differences in the determinations of V_{ub} and V_{cb} be explained by New Physics?*, *Phys. Rev. Lett.* **114** (2015) 011802 [arXiv:1407.1320] [INSPIRE].

JHEP08(2022)039

[3] A.V. Manohar and M.B. Wise, *Heavy quark physics*, in *Cambridge Monographs on Particle Physics, Nuclear Physics and Cosmology* **10**, Cambridge University Press, Cambridge, U.K. (2000).

[4] D. Benson, I.I. Bigi, T. Mannel and N. Uraltsev, *Imprecated, yet impeccable: On the theoretical evaluation of* $\Gamma(B \to X_c \ell \nu)$, *Nucl. Phys. B* **665** (2003) 367 [hep-ph/0302262] [INSPIRE].

[5] C.W. Bauer, Z. Ligeti, M. Luke, A.V. Manohar and M. Trott, *Global analysis of inclusive B decays*, *Phys. Rev. D* **70** (2004) 094017 [hep-ph/0408002] [INSPIRE].

[6] P. Gambino and C. Schwanda, *Inclusive semileptonic fits, heavy quark masses, and* V_{cb}, *Phys. Rev. D* **89** (2014) 014022 [arXiv:1307.4551] [INSPIRE].

[7] A. Pak and A. Czarnecki, *Heavy-to-heavy quark decays at NNLO*, *Phys. Rev. D* **78** (2008) 114015 [arXiv:0808.3509] [INSPIRE].

[8] K. Melnikov, $O(\alpha_s^2)$ *corrections to semileptonic decay* $b \to c\ell\bar{\nu}$, *Phys. Lett. B* **666** (2008) 336 [arXiv:0803.0951] [INSPIRE].

[9] S. Biswas and K. Melnikov, *Second order QCD corrections to inclusive semileptonic* $b \to X_c \ell \bar{\nu}$ *decays with massless and massive lepton*, *JHEP* **02** (2010) 089 [arXiv:0911.4142] [INSPIRE].

[10] P. Gambino, *B semileptonic moments at NNLO*, *JHEP* **09** (2011) 055 [arXiv:1107.3100] [INSPIRE].

[11] T. Becher, H. Boos and E. Lunghi, *Kinetic corrections to* $B \to X_c \ell \bar{\nu}$ *at one loop*, *JHEP* **12** (2007) 062 [arXiv:0708.0855] [INSPIRE].

[12] A. Alberti, T. Ewerth, P. Gambino and S. Nandi, *Kinetic operator effects in* $\bar{B} \to X_c l \nu$ *at* $O(\alpha_s)$, *Nucl. Phys. B* **870** (2013) 16 [arXiv:1212.5082] [INSPIRE].

[13] A. Alberti, P. Gambino and S. Nandi, *Perturbative corrections to power suppressed effects in semileptonic B decays*, *JHEP* **01** (2014) 147 [arXiv:1311.7381] [INSPIRE].

[14] M. Fael, T. Mannel and K. Keri Vos, V_{cb} *determination from inclusive* $b \to c$ *decays: an alternative method*, *JHEP* **02** (2019) 177 [arXiv:1812.07472] [INSPIRE].

[15] T. Mannel, D. Moreno and A.A. Pivovarov, *NLO QCD corrections to inclusive* $b \to c\ell\bar{\nu}$ *decay spectra up to* $1/m_Q^3$, *Phys. Rev. D* **105** (2022) 054033 [arXiv:2112.03875] [INSPIRE].

[16] M. Fael, K. Schönwald and M. Steinhauser, *Third order corrections to the semileptonic* $b \to c$ *and the muon decays*, *Phys. Rev. D* **104** (2021) 016003 [arXiv:2011.13654] [INSPIRE].

[17] M. Fael, K. Schönwald and M. Steinhauser, *Kinetic Heavy Quark Mass to Three Loops*, *Phys. Rev. Lett.* **125** (2020) 052003 [arXiv:2005.06487] [INSPIRE].

[18] M. Fael, K. Schönwald and M. Steinhauser, *Relation between the* $\overline{MS}$ *and the kinetic mass of heavy quarks*, *Phys. Rev. D* **103** (2021) 014005 [arXiv:2011.11655] [INSPIRE].

[19] M. Dowling, J.H. Piclum and A. Czarnecki, *Semileptonic decays in the limit of a heavy daughter quark*, *Phys. Rev. D* **78** (2008) 074024 [arXiv:0810.0543] [INSPIRE].

[20] I.I.Y. Bigi, M.A. Shifman, N. Uraltsev and A.I. Vainshtein, *High power n of* m_b *in beauty widths and* $n = 5 \to \infty$ *limit*, *Phys. Rev. D* **56** (1997) 4017 [hep-ph/9704245] [INSPIRE].

[21] A. Czarnecki, K. Melnikov and N. Uraltsev, *NonAbelian dipole radiation and the heavy quark expansion*, *Phys. Rev. Lett.* **80** (1998) 3189 [hep-ph/9708372] [INSPIRE].

[22] M. Beneke and V.A. Smirnov, *Asymptotic expansion of Feynman integrals near threshold*, *Nucl. Phys. B* **522** (1998) 321 [hep-ph/9711391] [INSPIRE].

JHEP08(2022)039

[23] V.A. Smirnov, *Analytic tools for Feynman integrals*, in *Springer Tracts in Modern Physics*, Springer, Berlin, Germany (2012).

[24] M. Czakon, A. Czarnecki and M. Dowling, *Three-loop corrections to the muon and heavy quark decay rates*, *Phys. Rev. D* **103** (2021) L111301 [arXiv:2104.05804] [INSPIRE].

[25] A. Pak and A. Smirnov, *Geometric approach to asymptotic expansion of Feynman integrals*, *Eur. Phys. J. C* **71** (2011) 1626 [arXiv:1011.4863] [INSPIRE].

[26] F. Herren, *Precision Calculations for Higgs Boson Physics at the LHC. Four-Loop Corrections to Gluon-Fusion Processes and Higgs Boson Pair-Production at NNLO*, Ph.D. Thesis, KIT, Karlsruhe, Germany (2020) [https://doi.org/10.5445/IR/1000125521].

[27] R.N. Lee and V.A. Smirnov, *Analytic ϵ-expansions of Master Integrals Corresponding to Massless Three-Loop Form Factors and Three-Loop $g-2$ up to Four-Loop Transcendentality Weight*, *JHEP* **02** (2011) 102 [arXiv:1010.1334] [INSPIRE].

[28] B. Ruijl, T. Ueda and J. Vermaseren, *FORM version 4.2*, arXiv:1707.06453 [INSPIRE].

[29] A.V. Smirnov and F.S. Chuharev, *FIRE6: Feynman Integral REduction with Modular Arithmetic*, *Comput. Phys. Commun.* **247** (2020) 106877 [arXiv:1901.07808] [INSPIRE].

[30] R.N. Lee, *Presenting LiteRed: a tool for the Loop InTEgrals REDuction*, arXiv:1212.2685 [INSPIRE].

[31] S.A. Larin, *The Renormalization of the axial anomaly in dimensional regularization*, *Phys. Lett. B* **303** (1993) 113 [hep-ph/9302240] [INSPIRE].

[32] S.A. Larin and J.A.M. Vermaseren, *The α_s^3 corrections to the Bjorken sum rule for polarized electroproduction and to the Gross-Llewellyn Smith sum rule*, *Phys. Lett. B* **259** (1991) 345 [INSPIRE].

[33] S.M. Berman and A. Sirlin, *Some considerations on the radiative corrections to muon and neutron decay*, *Ann. Phys.* **20** (1962) 20.

[34] M. Roos and A. Sirlin, *Remarks on the radiative corrections of order α^2 to muon decay and the determination of G_μ*, *Nucl. Phys. B* **29** (1971) 296 [INSPIRE].

[35] https://www.ttp.kit.edu/preprints/2022/ttp22-028/.

[36] A. Alberti, P. Gambino, K.J. Healey and S. Nandi, *Precision Determination of the Cabibbo-Kobayashi-Maskawa Element V_{cb}*, *Phys. Rev. Lett.* **114** (2015) 061802 [arXiv:1411.6560] [INSPIRE].

[37] M. Bordone, B. Capdevila and P. Gambino, *Three loop calculations and inclusive V_{cb}*, *Phys. Lett. B* **822** (2021) 136679 [arXiv:2107.00604] [INSPIRE].

[38] BELLE collaboration, *Measurements of q^2 Moments of Inclusive $B \to X_c \ell^+ \nu_\ell$ Decays with Hadronic Tagging*, *Phys. Rev. D* **104** (2021) 112011 [arXiv:2109.01685] [INSPIRE].

[39] BELLE collaboration, *Moments of the electron energy spectrum and partial branching fraction of $B \to X_c e \nu$ decays at Belle*, *Phys. Rev. D* **75** (2007) 032001 [hep-ex/0610012] [INSPIRE].

[40] P. Gambino, K.J. Healey and S. Turczyk, *Taming the higher power corrections in semileptonic B decays*, *Phys. Lett. B* **763** (2016) 60 [arXiv:1606.06174] [INSPIRE].

[41] DELPHI collaboration, *Determination of heavy quark non-perturbative parameters from spectral moments in semileptonic B decays*, *Eur. Phys. J. C* **45** (2006) 35 [hep-ex/0510024] [INSPIRE].

[42] J.A.M. Vermaseren, *Axodraw*, *Comput. Phys. Commun.* **83** (1994) 45 [INSPIRE].

[43] D. Binosi and L. Theussl, *JaxoDraw: A Graphical user interface for drawing Feynman diagrams*, *Comput. Phys. Commun.* **161** (2004) 76 [hep-ph/0309015] [INSPIRE].

JHEP08(2022)039